PHOTO-CATALYTIC DEGRADATION OF DYE BY ZINC OXIDE BASED CATALYST

A DISSERTATION

Submitted in partial fulfillment of the

requirements for the award of the degree

of

MASTER OF TECHNOLOGY

in

CHEMICAL ENGINEERING

(With Specialization in Industrial Pollution Abatement)

By

PRIYANKA

DEPARTMENT OF CHEMICAL ENGINEERING

INDIAN INSTITUTE OF TECHNOLOGY ROORKEE

ROORKEE-247667 (INDIA)

JUNE 2013

CANDIDATE'S DECLARATION

I hereby declare that the work being presented by me in this dissertation entitled **"PHOTO-CATALYTIC DEGRADATION OF DYE BY ZINC OXIDE BASED CATALYST**" in the partial fulfillment of the requirements for the award of the degree of Master of Technology in Chemical Engineering with specialization in "Industrial Pollution Abatement" submitted to the Department of Chemical Engineering, Indian Institute of Technology Roorkee, Roorkee, is an authentic record of my original work carried out under the guidance of **Dr. V.C. Srivastava**, Assistant Professor, Department of Chemical Engineering, IIT Roorkee. The matter embodied in this project report has not been submitted for the award of any other degree.

Date: 14 June, 2013 Priyanka

Place: Roorkee Enrol. No: 11515014

CERTIFICATE

This is to certify that the above statement made by the candidate is correct to the best of my knowledge.

(**V. C. Srivastava**)
Assistant Professor,
Department of Chemical Engineering
Indian Institute of Technology, Roorkee
Roorkee-247667

ACKNOWLEDGEMENTS

I am greatly indebted to my esteemed guide, **Dr. V.C. Srivastava**, Assistance Professor, Department of Chemical Engineering, Indian Institute of Technology Roorkee for his kind support and guidance during the entire course of this work. His cooperation and in depth knowledge have made my work possible. I am thankful to **Prof. Indra Deo Mall**, Department of Chemical Engineering for his inspiring guidance. His infallible supervision and guidance has made this work a more rewarding experience for me.

I am thankful to **Prof. V.K. Agarwal**, Head, Department of Chemical Engineering and other staff members for their instant help in all kinds of work.

I would like to thank **Mr. R. Bhatnagar and other research scholars** of PAR Lab, Department of Chemical Engineering, Indian Institute of Technology Roorkee.

I would like to thank my friends for their continuous support and enthusiastic help.

Last but not least, it is owed to the blessing of my parents and God that I have come up with this work in due time.

PRIYANKA

(11515014)

ABSTRACT

In the present study, photocatalytic oxidation of dye bearing wastewater has been done using iron doped zinc oxide photocatalyst. Various iron doped zinc oxide (Fe/ZnO) photocatalysts were synthesized by solution combustion synthesis method and its structural, morphological and optical properties were studied using N_2 adsorption-desorption, fourier transform infrared spectroscopy (FTIR), X-ray diffractometer (XRD), thermogravimetric analysis (TGA) , field emission scanning electron microscope (FE-SEM), transition electron microscope (TEM), energy dispersive analysis of X-rays spectroscopy (EDAX), and UV-visible diffuse reflectance spectra (UV-DRS). Synthesized catalyst activity was monitored by optimizing reaction parameters of photocatalytic oxidation process. XRD patterns of all samples showed a hexagonal wurtzite structure. The diffuse reflectance spectra of the prepared samples have shown the maximum absorption of light in the UV region stating that these catalysts can be used as photocatalysts.Using tauc plots band gap energies of all samples were determined and have values in the range of 3.14-3.38 eV. The BET surface area analysis of photocatalyst showed a good value of surface area to treat the dye solution. The presence of pronounced hysteresis in N_2 adsorption-desorption isotherm curves indicated the three dimensional network arrangement of the pores in the Fe/ZnO sample prepared using solution combustion synthesis method. The photodegradation ability of the catalysts were tested for the photodegradation of an azo dye named as acid red 1 dye. . Effect of various reaction parameters such as amount of iron doped, calcination temperature, calcination time, pH of dye solution, catalyst dose, hydrogen peroxide dose, reaction temperature and initial concentration of dye solution were optimized by taking color removal and degradation of dye as response. At optimum conditions, more that 71% color removal and 94% dye degradation was observed for acid red 1 dye solution having initial concentration of 50 mg/l and initial color 2730 Pt:Co units.

NOMENCLATURE

r	Rate of reaction, particle radius (m)
K_1	Langmuir adsorption constant
k	Reaction rate constant
A_0	Absorbance of dye
A	Absorbance of dye after treatment
C_0	Initial concentration of dye
C	Concentration of dye after treatment
I_0	Incident light intensity
I	Light intensity after passing through the sample
A	Absorbance coefficient
λ_m	Maximum wavelength (nm)
R^2	Goodness of fit
λ	Wavelength (nm)
h	Plank's constant (J s/photon)
c	Speed of light (m/s)
t	Reaction time (min)
D	Crystallite size (nm)
K	Scherrers constant
B	Forward width at half maximum (FWHM) (radian)
Θ	Half value of the Bragg diffraction angle (degree)
ϕ	Equivalence ratio
v	Frequency of the radiation
n	Exponent
E_g	Band gap energy
e^-_{CB}	Electron of conduction band
h^+	hole
A	proportional constant

LIST OF TABLES

Table 1.1 Characteristics of acid red 1 dye (Azophloxine) 4

Table 2.1 Literature survey on modification of transition metal doped zinc oxide (ZnO) photocatalyst 10

Table 2.2 Kinetics of various dyes studied.....13

Table 2.3 Optimum catalyst dosage for various dyes studied and the other process conditions. 16

Table 2.4 Range of pH studied and other operational parameters.....18

Table 2.5 Table 2.5 Range of oxidant studied and other operational parameters……..26

Table 2.6 Range or concentration of dyes investigated and their reaction volumes with the other process parameters. 21

Table 4.1 Physico-chemical characteristics of Catalysts 37

Table 4.2 Structural and crystallographic characteristics of both ZnO and Fe/ZnO catalyst 38

Table 4.3 Band gap energies of iron doped zinc oxide photocatalysts 39

List of figures

Figure 1.1 Different types of advanced oxidation processes.....4

Figure 3.1 Block diagram of the procedure to prepare the photocatalyst (Fe/ZnO).....26

Figure 3.2 Calibration curve of acid red 1 dye (Azophloxine).....26

Figure 3.3 Experimental set-up for photocatalytic oxidation of Azo dye (acid red 1) dye....27

Figure 4.1 Adsorption/desorption isotherms of N_2 at 77K on Fe/ZnO.....39

Figure 4.2 Pore size distribution of 2.5wt% Fe/ZnO 40

Figure 4.3 FTIR spectra of (a) undoped and 2.5wt% iron doped ZnO, (b) Acid red 1 dye and 2.5wt% Fe/ZnO (after oxidation). 41

Figure 4.4 XRD patterns of undoped ZnO and 2.5wt% iron doped ZnO. 42

Figure 4.5 Differential thermal gravimetric analysis and differential thermal analysis of 2.5wt% Fe/ZnO.....42

Figure 4.7 EDS patterns of 2.5wt% Fe/ZnO (a) before oxidation, (b) after oxidation. 43

Figure 4.8(a) TEM images and (b) SAED patterns of 2.5wt% Fe/ZnO. 44

Figure 4.9 Changes in the UV–vis absorption spectra of acid red 1 dye with reaction time. 45

Figure 4.10 DRS spectra of iron doped ZnO particles.....45

Figure 4.11 Tauc plots of the undoped and iron doped samples. 46

Figure 4.12 Effect of concentration of dopant and calcination temperature on dye degradation and color removal of acid red 1 dye.....47

Figure 4.14 Effect of photocatalyst dosage on color removal and dye degradation.....48

Figure 4.15 (a) Effect of pH of dye solution, (b) zeta potential of acid red 1 dye on dye degradation, color removal.....49

Figure 4.16 Effect of Oxidant dosage on color removal and dye degradation.....49

Figure 4.17 Effect of Reaction temperature on color removal and dye degradation.....50

Figure 4.18 Effect of Initial concentration of dye on color removal and dye degradation 50

Figure 4.19 Time dependence of concentration and zeta potential of acid red 1 dye.....51

TABLE OF CONTENTS

Page No.

CANDIDATE'S DECLARATION **i**

ACKNOWLEDGEMENT **ii**

ABSTRACT **iii**

NOMENCLATURE **iv**

LIST OF TABLES **v**

LIST OF FIGURES **vi**

1. INTRODUCTION 1

1.1. GENERAL 1

1.2. DYES 1

1.3. TREATMENT PROCESSES 1

1.3.1. Advanced oxidation processes (AOPs) 2

1.4. HETEROGENEOUS PHOTOCATALYTIC OXIDATION 2

1.5. PHOTOCATALYST 3

1.6. OBJECTIVES OF THESIS 3

2. LITERATURE REVIEW OF ZnO MEDIATED PHOTOCATALYTIC DYE DEGRADATION 5

2.1. TYPE OF PHOTOCATALYTIC REACTORS AND THEIR CONFIGURATIONS 5

USED IN ZnO MEDIATED PHOTOCATALYTIC DYE DEGRADATION 5

2.2. KINETIC MODELS 5

2.3. FACTORS AFFECTING THE RATE OF DYE DEGRADATION 6

2.3.1. Effect of dopant concentration 6

2.3.2. Effect of calcination temperature and time 7
2.3.2. Effect of catalyst dosage 8
2.3.3. Effect of pH 8
2.3.4. Effect of oxidant 8
2.3.5. Effect of reaction temperature 9
2.3.6. Effect of initial concentration of dye 9
3. EXPERIMENTAL 23
3.1. MATERIALS 23
3.2. PREPARATION OF IRON DOPED ZINC OXIDE USING SOLUTION 23
COMBUSTION SYNTHESIS METHOD 23
3.4. PHOTO REACTOR AND EXPERIMENTAL CONDITIONS 25
4. RESULTS AND DISCUSSIONS 28
4.1. CHARACTERIZATION OF Fe/ZnO 28
4.1.1. Braumer-Emmett-Teller (BET) Surface area analysis 28
4.1.2. Thermogravimetric analysis 28
4.1.3. FTIR Analysis 29
4.1.4. Structural analysis of iron doped zinc oxide photocatalysts 29
4.1.5. Morphological analysis of photocatalyst 30
4.1.6. UV–vis spectrum studies 31
4.1.7. Optical studies of iron doped zinc oxide 31
4.2. EFFECTS OF VARIOUS PARAMETERS ON PHOTOCATALYTIC 32
DEGRADATION OF ACID RED 1 DYE 32
4.2.1. Effect of concentration of dopant 32
4.2.2. Effect of calcination temperature 33
4.2.3. Effect of calcination time 33

4.2.4. Effect of catalyst dosage 34
4.2.5. Effect of pH of dye 34
4.2.6. Effect of oxidant dosage 35
4.2.7. Effect of reaction temperature 35
4.2.8. Effect of initial concentration of dye 35
4.2.9. Effect of reaction time 36
5. CONCLUSION AND RECOMMENDATIONS 52
5.1. CONCLUSIONS 52
5.2. RECOMMENDATIONS 53
REFERENCES 54

1. INTRODUCTION

1.1. GENERAL

Dye bearing effluent water from dyeing, textile, pulp, and paper industries have been a growing concern for many years [Pandit and Basu, 2004]. According to the World Bank estimation, 17–20% of the industrial water pollution comes from textile dyeing and wastewater treatment [Riaz et al., 2012; Juang et al., 2010]. In the textile industry, various physical and chemical operations are used to obtain final product. These processes are responsible for many sub-products which generate along with main product and are discharged to water bodies [Chacon et al., 2005].

1.2. DYES

Wastewaters from textile industries contain considerable amounts of non-fixed dyes, especially azo-dyes, and a huge amount of inorganic salts [Riaz et al., 2012]. Azo dyes constitute 60–70% of all dyestuffs produced. [Carliell et al., 1994; Meric et al., 2004]. Dyes having one or more azo groups (R_1-N=N-R_2) and aromatic rings mostly substituted by sulfonate group (-SO_3), hydroxyl group (-OH) are referred as azo dyes [Neill et al., 2000; Rajaguru et al., 2000].

Acid red 1 dye also known as Azophloxine, is one of the toxic and stable azo dye and widely used for the dying purpose. It is also used for the determination of proteins and peptides [Biçer and Arat, 2009]. Prolonged or repeated exposure to acid red 1 dye may cause allergic reactions in certain sensitive individuals. Chemical structure and properties of acid red 1 dye are given in Table 1.1.

1.3. TREATMENT PROCESSES

Textile dyes in wastewater are not only a source of non-aesthetic pollution but are a concern of health hazards as well. Therefore, it is very crucial to investigate suitable techniques to remove these harmful Azo dyes from wastewater [Sweeny et al., 1994].

Dye bearing wastewater can be treated using several methods (such as adsorption, electrochemical, flocculation-precipitation, physicochemical and biological). But the major disadvantage of these methods is that they basically do not degrade the pollutants completely, they only transfer them from the liquid phase to the solid or another liquid phase and produce a secondary pollution that requires very costly disposal [Gupta et al., 2006]. Biological methods are considered as more environmentally friendly and easier to apply on dye bearing wastewater,

but the production of sludge proportionally to the volume of treated water is a major drawback of biological methods. Recycling is essential if the volume to be treated is huge, [Silva et al., 2006 and Juang et al., 2010]. Chemical reactions with chlorine or coagulation techniques introduce harmful chemicals that are released into the environment [Hashimoto et al., 2005].

1.3.1. Advanced oxidation processes (AOPs)

Advanced oxidation processes (AOPs) appear to be more promising method to treat dye bearing wastewater [Faisal et al., 2007]. In AOPs, pollutant can be easily degraded at ambient temperature and pressure by the generation of highly reactive radicals [Glaze et al., 1987], Hydroxyl radicals are very fast and effective reactive species that attack on organic matter present wastewater and convert into less harmful products like carbon di-oxide and water. As hydroxyl radicals are so reactive and unstable, they must be continuously produced by means of photochemical or chemical reactions [Kusvuran et al., 2004]. Various types of AOPs are based on the medium of hydroxyl radical formation and are shown in Figure 1.1.

1.4. HETEROGENEOUS PHOTOCATALYTIC OXIDATION

Heterogeneous photocatalysis has been extensively investigated in recent years for the removal of toxic organic pollutants present in industrial effluent [Sanchez et al., 2011]. This method does not only degrades the pollutants but also causes complete mineralization of organic pollutants to CO_2, H_2O, and mineral acids [Hashimoto et al., 2005; Gupta et al., 2006; Lathasree et al., 2004]. In heterogeneous photocatalytic oxidation process, reaction takes place on the semiconductor surface under appropriate irradiation to form electron/hole pairs (e^-/h^+) [Riaz et al., 2012]. Hydroxyl radicals are produced by the reaction of hole present in the valence band with the water absorbed at the surface of semiconductor and the e^- in the conduction band reduces absorbed oxygen to form peroxide radicals anions (O_2^-) that further reacts with hydrogen peroxide to form hydroxyl radicals [Pera-Titus et al., 2004; Fujishima et al., 2000].

The most widely postulated reactions are:

$$H_2O_2 \rightarrow OH^- \quad (1.1)$$

$$OH^- + h^+ \rightarrow OH^\bullet \quad (1.2)$$

$$O_2 + e^- \rightarrow O_2^- \quad (1.3)$$

$$H_2O_2 + O_2^- \rightarrow 2OH^\bullet \quad (1.4)$$

1.5. PHOTOCATALYST

The semiconductors are used as photocatalyst due to their non-toxicity, low cost and insolubility under most environmental conditions [Sanchez et al., 2011]. Various metal oxide semiconductors (i.e., ZnO, TiO_2, WO_3 and SnO_2) have been studied as photocatalyst [Shinde et al., 2012]. TiO_2 is a promising photocatalyst due to its low band gap energy (3.2 eV), abundant availability, cost-effectiveness and chemical stability [Juang et al., 2010]. ZnO has been reported as suitable alternative to TiO_2 due to having similar band gap energy and photodegradation mechanism as TiO_2. ZnO absorbs over a larger fraction of the UV spectrum and absorbs more light quanta than TiO_2 and that increases its photocatalytic efficiency compared with TiO_2 in the degradation of several organic contaminants [Sun et al., 2010]. But the photocatalyst needs to be further improved to avoid the fast recombination rate of the photogenerated electron/hole pairs and un-utilization of solar spectrum due to wide band gap [Shi et al., 2011]. Doping of metal ion on semiconductor photocatalyst prevents the recombination of electron/hole pair and extends its light absorption region [Asilturk et al., 2009]. Photocatalysts can be prepared using several methods: Solution combustion synthesis method, Microemulsion preparation method, Ultrasound-assisted impregnation- calcination method, Solvothermal treatment method, Sol-gel method, Wet impregnation, Complex precipitation, Deposition precipitation

1.6. OBJECTIVES OF THESIS

The objective of this study is to investigate the photocatalytic oxidation of acid red 1 dye present in textile wastewater using Fe/ZnO, as a photocatalyst. The following objectives were set for the present work.

1. To synthesize iron doped zinc oxide (Fe/ZnO) by solution combustion synthesis process.
2. To carry out detailed characterization of catalyst for studying its various properties. These characterization techniques include X-ray diffraction (XRD), Thermogravimetric analysis (TGA), Field Emission-Scanning Electron Microscopy (FE-SEM), Braumer-Emmett-Teller analysis (BET), UV-Vis diffuse reflectance spectroscopic (UV-DRS), Transition electron microscopy (TEM), and Fourier transform infrared spectral (FTIR) analysis.
3. To study the degradation of acid red 1 dye present in textile waste water in the presence of UV light radiation using (Fe/ZnO), as a photocatalyst in a batch photo oxidation reactor
4. To optimize the preparation conditions and operational parameters affecting photocatalytic oxidation of azo dye.

Table 1.1 Characteristics of acid red 1 dye (Azophloxine) [Safety data sheet, sigma-aldrich.com]

Chemical structure	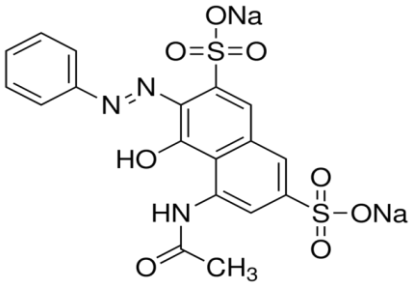
Synonyms	Azophloxine, Food Red 10, Amido Naphthol Red G
Empirical Formula	$C_{18}H_{13}N_3Na_2O_8S_2$
Molecular Weight	509.42
Color	Red
Potential health effects	
Inhalation	May be harmful if inhaled, may cause respiratory tract irritation.
Ingestion	May be harmful if swallowed.
Skin	May be harmful if absorbed through skin, may cause skin irritation.
Eyes	May cause eye irritation.

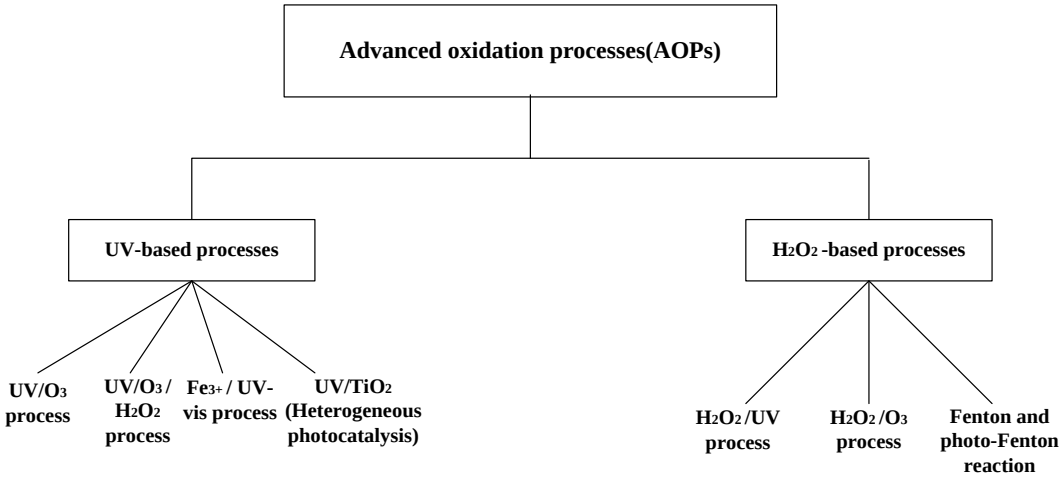

Figure 1.1 Different types of advanced oxidation processes [Rodríguez M, 2003]

2. LITERATURE REVIEW OF ZnO MEDIATED PHOTOCATALYTIC DYE DEGRADATION

In this chapter, literature review on the photocatalytic oxidation of dye from wastewater using Fe/ZnO is presented. Various zinc oxide based catalyst have been reported in literature and their photo degradability have tested and reported.

2.1. TYPE OF PHOTOCATALYTIC REACTORS AND THEIR CONFIGURATIONS USED IN ZnO MEDIATED PHOTOCATALYTIC DYE DEGRADATION

Reactors are very necessary to treat any type of wastewater and reactors can be of two type: batch and continuous reactor. Designing of reactor for the treatment of wastewater required kinetic data of the corresponding wastewater. In addition to the kinetic data, several aspects such as optimization and operation of photocatalytic reactors show a considerable effect on the dye degradation. Reactors needed for photocatalytic degradation were classified based on their design characteristics by [Lasa et al., 2004]. First classification is based on the state of photocatalyst; photocatalytic slurry reactors and reactors with immobilized photocatalyst. Second classification is based on type of light source; reactors with UV light radiation and reactors using solar light. Last classification is based on position of light source; reactors with immersed light source, reactors with external light source and reactors with distributed light source.

2.2. KINETIC MODELS

To analyze the heterogeneous photocatalytic reaction, Langmuir–Hinshelwood (L–H) kinetic expression has been used by many authors. For describing solid–liquid reaction and where surface controlled phenomena are observed L–H kinetic model is used to explain the kinetics [Jamil et al., 2012; Sobana and Swaminathan, 2007].The rate of degradation of dye at the surface is proportional to the coverage of catalyst surface by dye molecules. Table 2.1 includes a study on reaction kinetics given by several researchers along with the other process conditions.

The L-H expression is given as:

$$r = -\frac{dC}{dt} = \frac{K_1 kC}{1 + K_1 C} \qquad (2.1)$$

Where, C represents the concentration of the dye at any time‘t’, k represents the reaction rate constant and K_1 represents the Langmuir adsorption constant. Equation (2.1) can be linearized in to equation (2.2) to obtain the constants of the equation (2.1)

$$\frac{1}{r} = \frac{1}{k} + \frac{1}{K_1 kC} \tag{2.2}$$

If the term $K_1C \geq 1$, the equation 2.2 reduces to

$$r = K_1 kC \tag{2.3}$$

Equation (2.3) further can be expressed as

$$\ln\left(\frac{C_0}{C}\right) = K_1 kt = kt \tag{2.4}$$

Where, k is the apparent rate constant.

2.3. FACTORS AFFECTING THE RATE OF DYE DEGRADATION

The rate of dye degradation mainly depends upon number of hydroxyl radicals. So for achieving a good degradation rate, generation of hydroxyl radicals are very necessary. Whereas, generation of hydroxyl radicals is affected by various factors and these factors are briefly discussed in following section.

2.3.1. Effect of dopant concentration

Now a days, ZnO based photocatalysts has been given much importance due to its low cost, having high active sites, high surface area, nature of absorbing large fraction of UV spectrum and environmental safety [Kong et al., 2009; Fu et al., 2011]. With these advantages, ZnO has many drawbacks like fast recombination of electron hole pair because of large band gap energy (3.37 eV), low quantum yield in aqueous solution [Kong et al., 2009], poor absorbance of visible light spectrum [Wu et al., 2011].

In order to suppress the recombination of electron-hole pair and to decrease the band gap energy of ZnO, doping of transition elements is done. Transition metals such as Ni, Cr, Sn, Fe, etc. can be easily doped because of having similar ionic radii.

2.3.2. Effect of calcination temperature and time

Heat treated temperature/calcination temperature and time often affect the particle size, crystal size, band gap energy, surface area, crystal grade and other surface properties of photocatalyst. To determine the photocatalytic activity of semiconductor photocatalysts, calcination temperature and time play very important role [Wang et al., 2009; Wang et al., 2010]. Generally, TiO_2 are occurred in three crystal forms; anatase phase, rutile and brookite phase in which anatase phase shows high photocatalytic activity.TiO_2 often represents the converts from rutile phase to non-catalytic rutile phase under high calcination temperature and time. In case of ZnO, calcination step can be skipped because not all ZnO powders need calcination but only some needs the calcination to attain the high crystal grade. Some researchers have studied the effect of the calcination temperature and time on degradation rate of dye bearing wastewater.

Wang et al. [2009] achieved the maximum degradation of the acid red B dye using the Er^{3+}:$YAlO_3$/ZnO composite calcined at 500°C. They also calcined the catalyst at 300°C for 30 min but did not get good dye degradation because at low temperature crystallization was not done properly. They further varied the calcination time 30 to 60 and then 90 min. they found that photo degradability of catalyst is increasing with time upto 60 min but for 90 min, dye degradation is again decreasing because of probable occurrence of conglomeration of Er^{3+}:$YAlO_3$/ZnO particles. Fu et al. [2011] studied the degradation of methyl orange using copper doped zinc oxide and found that an increase in calcination time from 1 to 3 h, photocatalytic activity catalyst is enhanced but further increasing calcination time from 3 to 5 h, activity decreased drastically. From their finding, optimum calcination temperature was 350°C and time was 3 hr in order to have good degradation rate of dye bearing wastewater. Nagaraja et al. [2011] investigated the effect of crystal size on degradation efficiency of catalyst. They calcined the catalyst at three temperatures 600, 900 and 1000°C and found crystal size of 23,35 and 50 nm. They compared the photocatalytic activity of the as-prepared ZnO with that of calcined catalysts and found that calcined samples have poor photocatalytic activity because of increased diffusion path length and bulk recombination of charge carriers.

2.3.2. Effect of catalyst dosage

Catalyst loading is one of the major parameter to be studied in the process of heterogeneous catalysis [Muruganandham et al., 2006; Lu et al., 2009]. Catalyst loading affects the generation of hydroxyl radicals which converts organic dye molecules to non-toxic compounds [Nishio et al., 2006]. For a good degradation rate, optimum amount of catalyst is needed. Akyol and Bayramoglu [2005] studied the degradation of Remazol Red F3B and found that at higher catalyst loading, the catalyst particles were attenuated the light absorption into the reaction medium and results the lower degradation rates. Table 2.2 gives the optimum catalyst loading for the degraded dye along with the other process conditions.

2.3.3. Effect of pH

The effect of pH on the rate of photocatalytic degradation can be explained on the basis of dye adsorption onto the catalyst surface [Roselin et al., 2002] and zero point charge (ZPC) of the catalyst. Roselin et al. [2002] investigated the effect of pH on the decolorization as well as dye degradation of Remazol Red B dye. They observed that in acidic conditions, the rate of adsorption of the dye onto catalyst surface is high and the rate has been decreased when pH changed from acidic to basic. This may be because of ZPC of ZnO, has the value of about 10 [Akyol and Bayramoglu, 2005; Sobana and Swaminathan,2007; Lu et al.,2009]. Strong attractive forces occur between the dye molecules and the catalyst surface because the catalyst surface is positively charged below the ZPC value and negatively charged above the ZPC value. The range of pH studied along with other operational parameters are listed in Table 2.3.

2.3.4. Effect of oxidant

Generally, the use of oxidant is to promote the rate of degradation rate of dye bearing wastewater. Hasnat et al. [2007] and Pare et al. [2008] investigated the use of H_2O_2 as oxidant and the generation of $OH^{\cdot}$ radicals. H_2O_2 enhances the rate of degradation because it acts as electron acceptor (Eq.2.5), produces hydroxyl radicals by reacting with superoxide radical anion (Eq.2.6), and self decomposes under the illumination of UV light (Eq.2.7).

$$H_2O_2 + e^-_{CB} \rightarrow OH^- + OH^{\bullet} \quad (2.5)$$

$$H_2O_2 + O_2^{\bullet -} \rightarrow OH^- + OH^{\bullet} \quad (2.6)$$

$$H_2O_2 + 2h\nu \rightarrow 2\,OH^{\bullet} \quad (2.7)$$

Muruganandham et al. [2006] and Pare et al. [2008] investigated that use of excess oxidant suppress the degradation rate of dye bearing wastewater because of scavenging of hydroxyl radicals formed through photocatalytic process. Table 2.4 lists the range of oxidant used to study and along with the other process parameters.

2.3.5. Effect of reaction temperature

Tekbas et al. [2008] studied the decolorization of Remazol Brilliant Orange 3R dye at different temperatures such as 25, 30, 35, 40, 50 °C and found that Color removal was increased by increasing temperature. They reported that the temperature up to 40°C was easy to control but above this level heater was required to reach the temperature 50°C. Therefore, they took 35°C for further experiments. Sum et al. [2005] also studied the effect of temperature (in the range 30‑75 ◦C) on the degradation of azo-dye acid black 1. They reported that the initial TOC removal rate increases with reaction temperature and this may be because of an increase in collision frequency of molecules on the surface of the catalyst.

2.3.6. Effect of initial concentration of dye

Dye concentration affects the various parameters such as adsorptive, reactive, process, reaction kinetics and photo reactor design. Akyol and Bayramoglu, [2005] reported that rate of degradation of dye is enhanced by increasing the initial dye concentration according to the kinetics equation and as well as the surface reaction. From the rate expression it is evident that the increase in dye concentration gives higher degradation rates. But practically it is impossible because high concentration of dye obstructs the photons to strike the catalyst surface to produce hydroxyl radicals [Roselin et al., 2002; Nishio et al., 2006; Sobana and Swaminathan, 2007]. So photocatalytic degradation of dye depends upon interaction between light and catalyst surface. Table 2.5 gives the information containing the range of dye studied and the corresponding reaction volumes taken to study the influence of dye concentration.

Table 2.1 Literature survey on modification of transition metal doped zinc oxide (ZnO) photocatalyst.

Photocatalyst	Synthesis method	Type of dye	Degradation efficiency	References
SO_4^{2-}/ZnO/TiO_2	Modified sol–gel method using citric acid	methyl orange	71.9%	[Liao et al.,2004]
AC–ZnO	Mixing and stirring process	Direct blue 53	≈ 70%	[Sobana and Swaminathan, 2007]
Zinc oxide/carbon	Self-propagating solution combustion method	Not reported	Not reported	[Jayalakshmi et al., 2007]
ZnO	Not reported	AR18	≈ 100%	[Sobana and Swaminathan, 2007]
TiO_2-ZnO powders	Ultrasonic precipitation method	C.I. Basic Blue 41	≈ 100%	[Jiang et al.,2008]
Polymer modified ZnO	As given in literature	Rhodamine B, and methyl orange	100% and 40% respectively	[Qiu et al.,2008]
Er^{3+}:$YAlO_3$/ZnO–TiO_2	Ultrasonic dispersion and liquid boiling method.	Acid red B	90%	[Wang et al.,2009]
ZnO	Anodic deposition of ZnO thin film on zinc sheet	Cypermethrin	67.5%	[Ali et al.,2010]
ZnO/SiO_2	Chemical precipitation method	Rhodamine B	Different degradation ratios were reported	[Zhai et al.,2010]
$ZnCr_2O_4$	Sol–gel method	reactive blue 5 (RB5)	90%	[Yazdanbakhsh et al.,2010]
ZnO nanocrystals	Thermal decomposition of zinc oxalate	Reactive Red 120	95.8%	[Velmurugan; Swaminathan,

				2010]
ZnO	Sol–gel dip-coating method	Direct Yellow 12 (DY12)	98%	[Khataee et al.,2011]
Ag/AgCl/ZnO	Two-step synthesis method under the hydrothermal condition	Methyl orange	≈ 100%	[Xu et al.,2011]
Macroporous ZnO/MoO_3/SiO_2 hybrid	Sol–gel technology and biomimetic synthesis	Safranin T	95.4%	[Yuan et al.,2011]
Ag/tetrapod-like ZnO with different PEG contents	Photodeposition Method	Methyl orange	Different degradations were reported	[Wang et al., 2011]
Mn-doped ZnO	Microwave assisted hydrothermal synthesis process	Methyelene Blue	Not reported	[Mahmood et al., 2011]
Tin-doped ZnO	Room temperature solid-state reaction	methyl orange	≈80%	[Jia et al., 2011]
Sn-doped ZnO	Microwave heating method	Methylene Blue	80%	[Sun et al.,2011]
AgBr/ZnO	Chemical precipitation method	Methyl orange	≈ 100%	[Wu et al.,2012]
ZnO nanoparticles	Not reported	Acid red 27	≈70%	[Shanthi and Kuzhalosai, 2012]
Ag-doped zinc oxide	Spray pyrolysis Technique	Acid orange 7	99.5%	[Shinde et al.,2012]
Fe/ZnO/SiO_2	Sol-gel technique	Methylene Blue	≈ 100%	[Mohamed et al.,2012]

Nano-sized ZnO powder	Solution combustion synthesis method(SCS)	Rhodamine B	95%	[Nagaraja et al.,2012]
ZnO (Using Various Fuels)	Solution combustion synthesis method(SCS)	Orange G	Different degradations were reported	[Potti and Srivastava, 2012]
Different ZnO particles (rodlike, ricelike and disklike)	Sol–gel method	Rhodamine B	≈ 100%	[Pung et al.,2012]
Silver-Doped ZnO	Synthesized under mild hydrothermal conditions in the presence of surface modifiers	Brilliant blue FCF	94%	[Parvin et al.,2012]
ZnO suspension	Not reported	Acid red 73	≈ 100%	[Nilamadanthai et al.,2013]
Se doped ZnO nanoparticles	thermo-mechanical method	trypan blue	89%	[Nenavathu et al.,2013]
Ag-N-codoped zinc oxide nanoparticles	one-step impregnation method	Methyl red	61%(Under UV light), 92% (Under Solar light)	[Welderfael et al.,2013]

Table 2.2 Kinetics of various dyes studied

Catalyst	Type of dye	Kinetic study	References
ZnO	Eosin Y and Methylene Blue	Langmuir-Hinshelwood kinetics was used to describe the photo-oxidation kinetics	[Chakrabarti and dutta,2004]
ZnO	Orange II powder	Discussed the decolourization kinetics	[Nishio et al.,2006]
ZnO	Erythrosine and anionic textile dye	Discussed the decolourization kinetics	[Hasnat et al.,2007]
Ag:ZnO	Methyl orange	Pseudo first order reaction was observed and the rate constant for the degradation of MO was 1.9×10^{-1}/min	[Chen et al.,2008]
ZnO	Acridine orange	Investigated the kinetics for every operational factor which effects the dye degradation	[Pare et al.,2008]
ZnO	Direct yellow 12	Studied the kinetics analysis of dye degradation by fitting the data to the Langmuir-Hinshelwood kinetics expression	[Sivasankar and Sadasivam,2009]
Er^{3+}:$YAlO_3$ / ZnO	Acid red B	It was observed that the degradation reaction followed first order reaction kinetics under different conditions and the rate constants were found to be 0.0396 and 0.0190/ min respectively, for Er^{3+}:$YAlO_3$/ ZnO composite and for pure ZnO powder	[Wang et al.,2009]
2D-ZnO nanopellets	Methylene blue	Obtained different values of rate constants under different doses of catalyst	[Chiu et al.,2010]
Transition metal	Methylene blue	Determined the rate constant for each dopant and compared the degradation	[Barick et al.,2010]

doped ZnO nanoclusters		efficiencies	
ZnO	Methyl orange	Discussed the kinetic modeling with the powder ZnO photocatalyst and as well as ZnO film coated materials	Akyol and Bayramoglu,2010]
ZnO	Reactive red 120	Estimated the effect of operational parameter on the rate constant	[Velmurugan; Swaminathan,2010]
ZnO	Methylene blue	Estimated the rate constants for the prepared three different catalysts	[Gupta et al.,2011]
Ni:ZnO	Malachite green	Different rate constants were obtained with respect to the Ni doping percentage	[Kaneva et al.,2011]
Mn:ZnO	Methylene blue	Estimated the rate constants of dye degradation and compared with doped and undoped ZnO	[Mahmood et al., 2011]
ZnO	Acid violet 7	The rate constants was estimated for the degradation and expressed as a function of operational parameters	[Krishnakumar and Swaminathan,2011]
Zinc oxide microflowers	Methylene blue	The reaction rate constant was found to be 2.8×10^{-2}/min.	[Wahab et al.,2011]
ZnO	Brilliant golden yellow (BGY)	Estimated the Langmuir-Hinshelwood kinetics parameters as $k=1.01\times10^{5}$ l/mol and $K=0.32\times10^{5}$ mol/min.	[Habib et al.,2011]
Cu:ZnO	Methyl orange	The degradation reaction of MO followed the first order kinetics.	[Fu et al.,2011]
Co:ZnO	Methylene blue	Obtained rate constants for ZnO and doped ZnO as 0.119/min and 0.0538/min respectively.	[Nair et al.,2011]

CuO-ZnO Nano photo catalyst	Acid red 88	Obtained different rate constants for different oxidatns	[Satishkumar et al.,2011]
V:ZnO aerogel nano powder	Methylene blue	Obtained different apparent first order rate constants for different doping concentrations.	[Slama et al.,2011]
ZnO supported on montmorillonite	Methylene blue	Fitted to different isotherm models	[Fatimah et al.,2011]
TiO_2/AC	Methyl Orange	The photocatalytic degradation of MO dye obeys pseudo-first-order kinetics.	[Jamil et al., 2012]
Different ZnO particles(rodlike, ricelike and disklike)	Rhodamine B	First order kinetics was found and rate constant for rodlike, rice-like and disk-like particles are 0.06329 min^{-1}, 0.0431 min^{-1} and 0.02448 min^{-1} respectively.	[Pung et al.,2012]
Ag-N-codoped zinc oxide nanoparticles	Methyl red	Photocatalytic degradation of methyl red dye under UV and solar radiation follow pseudo first order kinetics	[Welderfael et al.,2013]

Table 2.3 Optimum catalyst dosage for various dyes studied and the other process conditions.

Dye	Catalyst dosage range studied(g/l)	Optimum dosage (g/l)	Dye concentration (mg/l or ppm)	pH	Reaction time(min)	References
Remazol red B	1-5	1	42.04	6.8	-	[Roselin et al.,2002]
Eosin Y and Methylene Blue	0.2-1.0 and 0.4-2.4	1.0 and 2.4	50	6.9	120	[Chakrabarti and dutta,2004]
Remazol Red F3B	0.15-0.75	0.6	150	7.0	10,30,60	Akyol and Bayramoglu ,2005]
OrangeII	0-10	2	7.31	7.7	200	[Nishio et al.,2006]
Direct blue 53	0.05-0.3	0.25	288.24	7.0	150	[Sobana and Swaminathan,2007]
Ethyl voilet	0-0.2	0.1	50	6	360	[Chen et al.,2007]
Acridine orange	0.1-0.35	0.25	5.31	-	120	[Pare et al.,2008]
Basic blue 11	0.025-0.1	0.05	50	-	1440	[Lu et al.,2009]
Direct yellow 12	0.25-1.25	0.75-1	34	7	20	[Rao et al.,2009]
Acid red B	0-0.125	0.1	10	Natural	60	[Wang et al.,2009]

Reactive red 120	0.1-0.2	0.2	294	5	30	[Velmuruga n; Swaminatha n,2010]
Acid violet 7	0.05-0.25	0.1	283.23	9	30	[Krishnaku mar and Swaminatha n,2011]
Brilliant golden yellow	0.005-0.15	0.05	20000	7.5	120	[Habib et al.,2011]
Rhodami ne B	-	0.2	10	-	80	[Nagaraja et al.,2012]
Rhodami ne B	-	0.5	-	-	80	[Pung et al.,2012]
Brilliant Blue	0.4-1.6	1.6	7.92	-	180	[Parvin et al.,2012]
Methyl red	-	0.2	-	-	40	[Welderfael et al.,2013]

Table 2.4 Range of pH studied and other operational parameters.

Dye	pH range studied	Dye concentration (mg/l or ppm)	Catalyst dosage (g/l)	Reaction time(min)	References
Remazol red B	3-12	42.04	3	-	[Roselin et al.,2002]
Methylene Blue	5.5-79.	50	0.4	120	[Chakrabarti and dutta,2004]
Remazol Red F3B	6-10	150	0.45	60	Akyol and Bayramoglu,2005]
OrangeII	3-11	10.2	1	180	[Nishio et al.,2006]
Erythrosine	5.5-10	6.15	0.025	125	[Hasnat et al.,2007]
Direct blue 53	3-12	288.24	0.25	60	[Sobana and Swaminathan, 2007]
Ethyl voilet	3-10	50	0.05	360	[Chen et al.,2007]
Acridine orange	3-7	5.31	0.25	180	[Pare et al.,2008]
Basic blue 11	3-10	50	0.05	1440	[Lu et al.,2009]
Direct yellow 12	4-10	34	0.75	70	[Rao et al.,2009]
Acid red B	3-11	10	0.1	60	[Wang et al.,2009]

Methylene Blue	5-12	10	0.05	20	[Kong et al.,2010]
Reactive red 120	3-11	294	0.2	30	[Velmurugan; Swaminathan, 2010]
Brilliant golden yellow	6-10	20000	0.05	120	[Habib et al.,2011]
Rhodamine B	2-12	10	-	80	[Nagaraja et al.,2012]
Brilliant Blue	2-12	7.92	1.6	180	[Parvin et al.,2012]

Table 2.5 Range of oxidant studied and other operational parameters.

Dye	**Range/concentration studied (M)**	**Dye concentration (m)×10^{-4}**	**Catalyst amount (g/l)**	**pH**	**Reaction time(min)**	**Oxidant**	**References**
Reactive black 5	0.01-0.05	3.85	-	3	210	H_2O_2	[Murugananndham et al.,2006]
Erythrosine	0.04	0.07	0.025	-	125	H_2O_2	[Hasnat et al.,2007]
Acridine orange	0.001-0.01	0.2	0.25	-	150	H_2O_2	[Pare et al.,2008]
Reactive red 120	0.01	2	0.2	5	30	Ozone	[Velmurugan; Swaminathan,2010]
Acid violet 7	0.0005,0.012,0.01	5	0.1	9	30	$H_3K_5O_{18}S_4$,$KBrO_3$, H_2O_2	[Krishnakumar and Swaminathan,2011]

Table 2.6 Range or concentration of dyes investigated and their reaction volumes with the other process parameters.

Dye	Concentration range studied(mg/l or ppm)	Reaction volume (ml)	Catalyst dosage(g/l)	pH	Reaction time(min)	References
Remazol red B	14-224	500	3	10	Continous process	[Roselin et al.,2002]
Eosin Y and Methylene Blue	25-60 and 25-100	400	0.4	6.9 and 7.5	120	[Chakrabarti and dutta,2004]
Remazol Red F3B	50-200	300	0.45	7.0	10,30,60	Akyol and Bayramoglu,2005]
OrangeII	4.08-27.6	2000	2	7.7	200	[Nishio et al.,2006]
Direct blue 53	96.08-864.07	50	0.25	7.0	150	[Sobana and Swaminathan,2007]
Acridine orange	2.65-13.27	50	0.25	-	180	[Pare et al.,2008]
Basic blue 11	50-200	100	0.05	9	1440	[Lu et al.,2009]
Direct yellow 12	6.8-40.8	250	-	-	80	[Rao et al.,2009]
Acid red B	5.0-25	100	0.1	Natural	60	[Wang et al.,2009]

Reactive red 120	147-588	50	0.2	5	30	[Velmurugan; Swaminathan,2010]
Acid violet 7	170-509.85	50	0.1	9	30	[Krishnakumar and Swaminathan,2011]
Brilliant golden yellow	5-60	50	0.05	7.5	150	[Habib et al.,2011]
Rhodamine B	10-30	100	0.2	-	80	[Nagaraja et al.,2012]

3. EXPERIMENTAL

3.1. MATERIALS

All the chemicals used in this study were of analytical grade. Acid red 1 dye (Chemport Private Limited, India), dextrose (S.D. Fine-Chem limited, India), ferric nitrate (S.D. Fine-Chem limited, India), zinc nitrate hexahydrate (HiMedia Laboratories Pvt. Ltd., India) and hydrogen peroxide (Merck specialties private limited, India) were purchased from various companies.

3.2. PREPARATION OF IRON DOPED ZINC OXIDE USING SOLUTION COMBUSTION SYNTHESIS METHOD

Iron doped zinc oxide (Fe/ZnO) was synthesized using solution combustion synthesis method. First stoichiometric amount of zinc nitrate hexahydrate, dextrose and ferric nitrate were taken in crucible and dissolved in minimum quantity of distilled water. Stoichiometric amount of the redox mixture was calculated using the total oxidizing (O) and reducing valences (F) of the reactants to keep equivalent ratio (φ_e) is unity (F/O=1). The valence of C, H, divalent and trivalent metal ions are + 4, +1, +2 and +3 respectively. The valence of the O is −2 and that the valence of nitrogen according to propellant chemistry is considered as zero. Thus, oxidizing valence of Zinc nitrate is −10 and reducing valence of dextrose ($C_6H_{12}O_6$) is +24. For the preparation of ZnO the required mole ratio of $ZnN_2H_{12}O_{12}$ to dextrose is 5: 12 [Nagaraja et al., 2012]. Solution was stirred for 30 min so as to form stoichiometric redox mixture. After stirring, solution was kept in preheated furnace at 400°C for 4-5 min. Required furnace temperature for dextrose can be roughly estimated using thermo gravimetric analysis (TGA) and differential thermal analysis (DTA). Another method to estimate furnace temperature is based on number of carbon atoms and type of functional groups of the fuel. A spark appears at one corner of mixture due to fuel present in redox mixture and results in an incandescent flame which spreads throughout the mass giving voluminous, fluffy and porous solid product. Solid product was then kept in desiccator for cooling and then fluffy solid mass was crushed to get it in amorphous form. Calcination of Fe/ZnO was done at different temperatures with different period to decompose the intermediates formed during reaction of dextrose and zinc nitrate. Block diagram of the procedure to prepare photocatalyst (Fe/ZnO) is shown in Figure 3.1. Photocatalyst was made of four different concentrations 1%, 2.5%, 5% and 7.5% in terms of mass percentage of iron.

Proposed synthesis reaction for preparation of iron doped zinc oxide using dextrose as a fuel:

$$ZnN_2H_{12}O_{12} + (5/12)\,C_6H_{12}O_6 \rightarrow ZnO + N_2 + (5/2)CO_2 + (17/2)\,H_2O$$

3.3. CATALYST CHARACTERIZATION

Surface area and porosity were determined by N_2 adsorption and desorption isotherms using Micromeritics ASAP 2020 instrument at -196 ^oC. Before analysis was performed, all samples were degassed at 150 ^oC to a vaccum 10^{-3} torr for 6 h. Surface area and micropore volume of samples were determined using the Brunauer–Emmett–Teller (BET) and t-plot equations, respectively, by assuming that all pores in the sample are cylindrical and parallel.

Fourier transform infrared (FTIR) spectrometer (Thermo Nicolet, USA) was employed to determine the chemical nature of iron doped zinc oxide a spectral range of 4000-400 cm^{-1}. The sample powder was pressed with KBr (1:300, wt: wt ratio) to achieve a reasonable signal-to-noise ratio.

XRD analysis was carried out by using Phillips (Holland) diffraction unit (Model PW1140/90) with copper as the target and nickel as the filter media. Radiation was maintained constant at 1.542 Å. Goniometric speed was maintained at 10°/min.

Differential thermal and thermo gravimetric analysis (DTA and TGA) experiment were carried out under air atmosphere at a flow rate of 200 ml/min in the temperature range of room temperature to 1000 ^oC with heating rate of 10 ^oC/min. Aluminum was used as a reference material and 8 mg of sample was placed in a ceramic crucible.

To understand the morphology of iron doped zinc oxide prepared from dextrose using solution combustion synthesis method, samples were gold sputter coated first and then Field emission-Scanning electron microscopy (FE-SEM) analysis was carried out using QUANTA200F. TEM analysis was also carried out to investigate the particle size of photocatalyst. A suspension of photocatalyst and ethanol is made and a drop this suspension was spread over a carbon-coated copper grid and after 15 min sonication, TEM images of photocatalyst particles were obtained.

UV-visible diffuse reflectance spectra (UV-DRS) of the copper loaded activated carbon was obtained in the UV region (200-600 nm) by a Shimadzu UV-2100 spectrometer with $BaSO_4$ as reference. The spectra were recorded at room temperature.

Concentration of Azo dye to calculate the dye degradation was determined by finding out the absorbance at the characteristic wavelength using a double beam UV-vis spectrophotometer (HACH, DR 5000, USA). Color of azo dye solution was measured in Pt:Co units using Aqualytic, Germany.

pH adjustments was carried out by HI 2211 pH/ORP meter and purchased from Hanna Instruments.

3.4. PHOTO REACTOR AND EXPERIMENTAL CONDITIONS

The experimental studies were carried out in a 250 ml beaker containing dye solution and catalyst was kept over magnetic stirrer. Magnetic stirrer was used to agitate the mixture and keep the solution homogeneous during the experimentation. The beaker was kept in cold water bath to cool the solution during experimental run. A thermometer was placed inside the solution to measure the temperature. The temperature of the reaction mixture was raised using the hot-plate to the desired value. A 125 watt UV bulb (365nm) was used for UV radiation and 250 ml beaker was kept under UV light for irradiation. UV bulb was suspended in such a manner so that the distance between the top of the reaction mixture and bulb should be about 8 cm. Magnetic stirrer, beaker and UV light were covered by a wooden box and that wooden box was covered by aluminum foil to avoid exposure of UV light. Figure 3.2 shows the experimental set-up designed for photocatalytic oxidation. In each run, the reactor was charged with 100 ml dye solution of required concentration with the required amount of photocatalyst (Fe/ZnO). Stirring of solution was done in dark for 30 min to establish adsorption-desorption equilibrium. After 30 min. required amount of oxidation agent (hydrogen peroxide) was added and UV light was switched on for 3 h [Nagaraja et al., 2012]. Vapors were carried out of the set-up by means of exhaust fan. Beginning of experiment was considered to occur simultaneously with the injection of hydrogen peroxide. After a predetermined time, dye solution was withdrawn and filtered, and then the concentration of dye solution was measured by (UV-Vis spectrophotometer, (SHIMADZU) and color of dye solution was measured in Pt:Co units (Aqualytic, Germany). Calibration curve of acid red 1 dye is shown in Figure 3.2. Percentage dye degradation and color of dye solution were calculated using following equations:

$$\text{Percentage dye removal} = \frac{(A_0 - A)}{A_0} 100 \qquad (3.1)$$

$$\text{Percentage color removal} = \frac{(C_0 - C)}{C_0} 100 \qquad (3.2)$$

Where, A_0 and A are the initial and final absorbance of dye solution; C_0 and C are the initial and final color of dye solution.

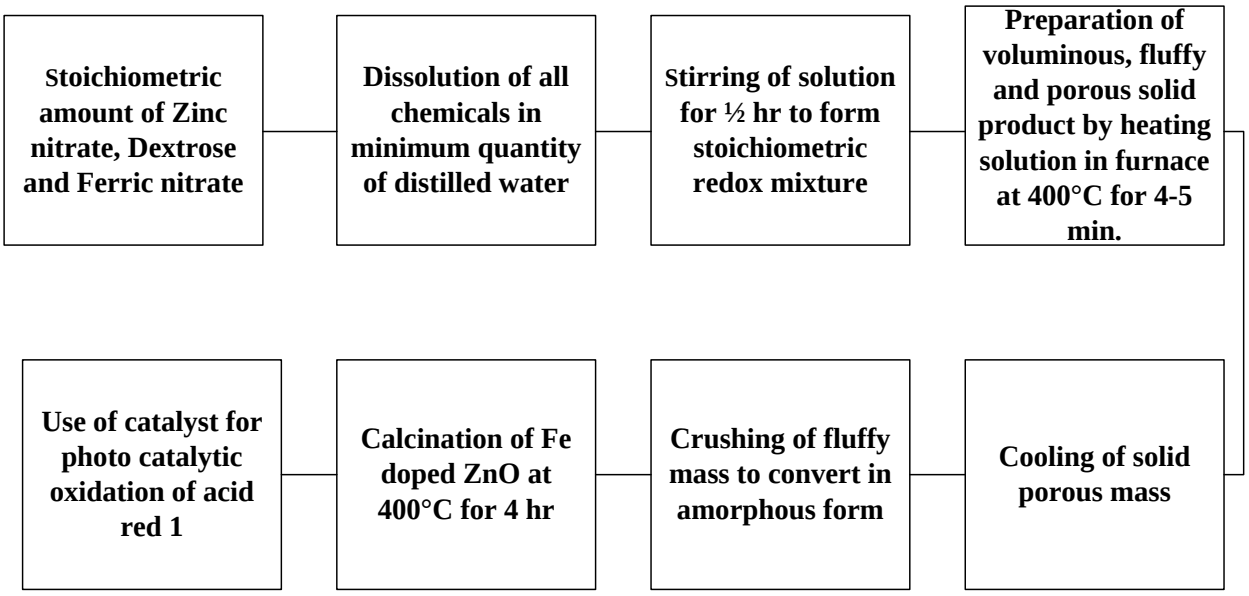

Figure 3.1 Block diagram of the procedure to prepare the photocatalyst (Fe/ZnO)

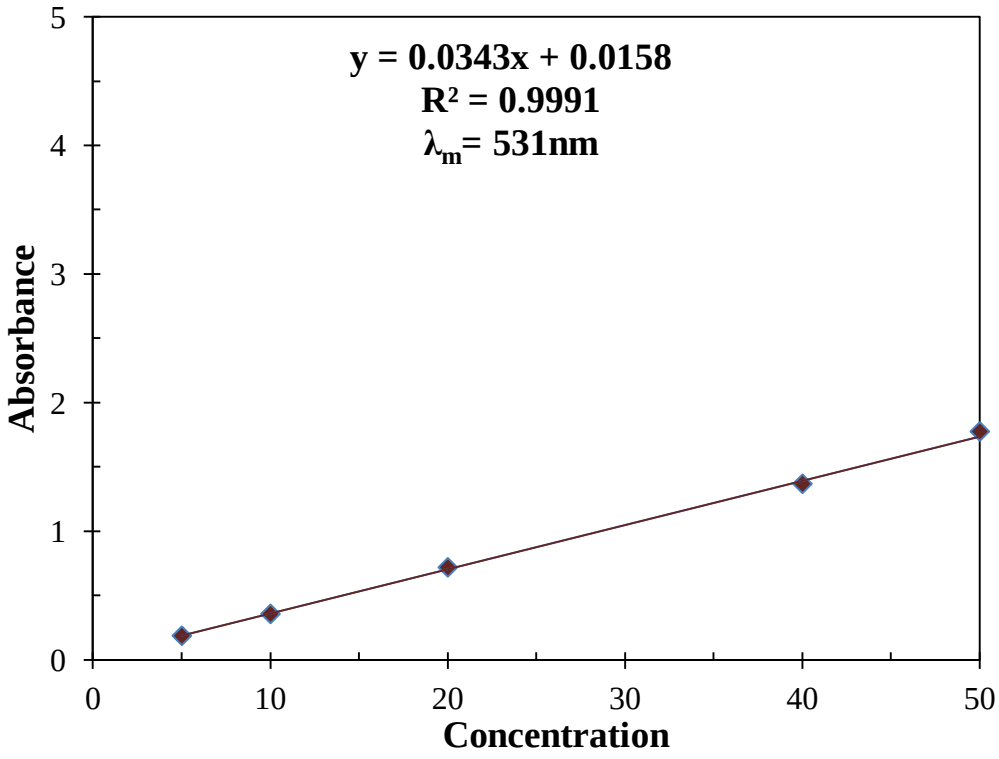

Figure 3.2 Calibration curve of acid red 1 dye (Azophloxine)

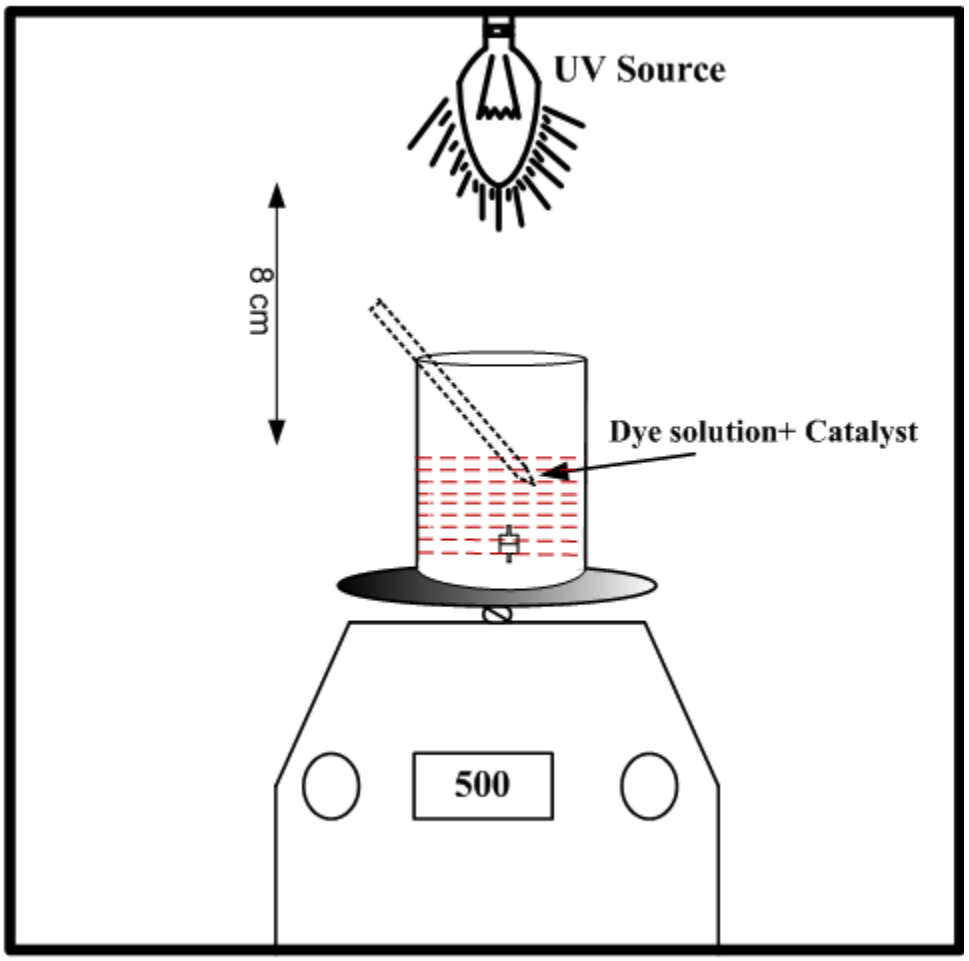

Figure 3.3 Experimental set-up for photocatalytic oxidation of Azo dye (acid red 1) dye

4. RESULTS AND DISCUSSIONS

4.1. CHARACTERIZATION OF Fe/ZnO

Results of the experiments on the preparation and characterization of iron doped zinc oxide (Fe/ZnO) are reported in this chapter. Optimization experiments results are also reported in this chapter.

4.1.1. Braumer-Emmett-Teller (BET) Surface area analysis

The physical or porous structure is of vital importance in understanding the oxidation process and the catalytic activity of a catalyst. The total pore volume was estimated from the liquid volume of the adsorbate (N_2) at 0.99 relative pressure. Prior to measurements, the samples were degassed under vacuum for 4 h and at the temperatures where they were synthesized. Physico-chemical characteristics of 2.5wt% Fe/ZnO are listed in Table 4.1. The isotherms of adsorption/desorption of N_2 at 77K on the Fe/ZnO is illustrated in Figure 4.1. The adsorbed volume increased with an increase in P/P_0, indicating a wider pore size distribution. The adsorption isotherm belongs to a mixture of type IV isotherms. According to IUPAC classification, the type IV isotherm indicates a mixture of micro-porous and mesoporous material [Srivastava et al., 2008]. The amount of nitrogen adsorbed smoothly increases up to p/p_0 =0.75 and the amount of nitrogen adsorbed rapidly increases and it reaches a maximum of 75-80 cm^3/g at p/p_0 = 0.9 [Jesionowski et al., 2011]. The structural heterogeneity of porous material is generally characterized in terms of the pore size distribution and pore size distribution is shown in Figure 4.2.

4.1.2. Thermogravimetric analysis

The thermogravimetric analysis curves (TGA and DTA) of Fe/ZnO are used to study the thermal stability of Fe/ZnO based on weight loss as a function of temperature and dispose spent-ZnO under inert and oxidizing atmosphere are shown in Figure 4.3 (a). Only one weight loss zone can be identified in the range of 25-400°C (6%) from the Figure 4.3 (a) and this wt loss is due to loss of moisture absorbed onto catalyst surface. After 400°C, no significant weight loss is found so this indicates the high thermal stability and high purity of nano ZnO(s) [Ghule et al., 2003]. Because of this factor catalyst was calcined at 400°C and gave best degradation. Thermogravimetric analysis of Fe/ZnO (after oxidation) is shown in Figure 4.3 (b) and shows higher weight loss of about 16% up to 400°C in comparison to freshly prepared Fe/ZnO due to

combustion of adsorbed dye molecules onto catalyst surface during photooxidation of dye. It can be concluded from Figure 3.3 (b) that iron doped zinc oxide can be reused because it is showing high thermal stability even after one use. In DTA study of the catalyst (before oxidation), no endothermic peak is observed indicating no phase change during the heating process, whereas an endothermic peak is observed between 200-270°C in DTA study of catalyst (after oxidation) indicating the decomposition of water and organic matter adsorbed onto catalyst surface and a change in crystal structure during heating [Raoufi,2013; Chen et al.,2008].

4.1.3. FTIR Analysis

The chemical structure of the catalyst surface affects the catalytic oxidation. Surface characteristics and surface behavior of the catalyst are influenced by carbon–oxygen functional groups. The FTIR spectra of the undoped ZnO, 2.5 wt% Fe/ZnO, Acid red 1 dye and 2.5wt% Fe/ZnO (after oxidation) is shown in Figure 4.4(a) and (b). The FTIR spectra of all samples were taken in the range of 400-4000 $cm^{-1.}$ The peak at 433 cm^{-1} in Figure 4.4(a) and (b) is due to stretching of Zn-O bond [Changlin et al., 2011]. The peaks from 3430-3480 and 1240-1230 cm^{-1} are attributed to surface hydroxyl groups in all samples and the peaks between 2910-2930 cm^{-1} are due to aliphatic CH. Small peaks are observed between 2350 -2360 cm^{-1} and these are attributed to the absorption of CO_2, evolved during combustion [Potti and Srivastava, 2012]. The stretching of C=O can be observed in all samples between 1750-1735 cm^{-1} and the peaks between 1630-1600 cm^{-1} are due to stretching vibration of C=C bond [Yuan et al., 2011]. Peaks between 1380-1370 cm^{-1} are due to $-CH_3$ stretching and the peaks between are the peaks between 1040-1050 cm^{-1} are attributed to stretching of aliphatic ether. From Figure 4.4(a) and (b) it can be concluded that doping of iron on ZnO is increasing the amount of functional groups present and no extra group is being added due to doping of iron. In Figure 4.4(a) and (b), no extra peak can be seen in iron doped ZnO after oxidation of dye and this may be because of total oxidation of organic matter present in dye solution.

4.1.4. Structural analysis of iron doped zinc oxide photocatalysts

XRD patterns of ZnO and 2.5 wt% iron doped ZnO is shown in Figure 4.5. The identification of all the peaks of both samples was done by comparing the peaks with joint committee on powder diffraction data (JCPDS) files (PDF: 800075). Both undoped and the doped samples posses hexagonal wurtzite structure and have no impurity phase, thus both samples are found in pure form and zinc oxide sample is successfully doped with iron.

XRD pattern of pure ZnO shows a series of characteristics peaks: 2.82, 2.62, 2.49, 1.92, 1.64, 1.48 and 1.38 whereas, XRD pattern of Fe/ZnO shows a series of characteristics peaks: 2.82,2.62, 2.48, 1.90, 1.63, 1.48 and 1.36. The peaks corresponding to 2.49 and 2.48 showed highest intensity for ZnO and Fe/ZnO photocatalyst respectively. From Figure 4.5, it can be seen that crystallinity of catalyst has decreased after doping of iron. Structural and crystallographic characteristics of both ZnO and Fe/ZnO catalyst are given in Table 4.2.

4.1.5. Morphological analysis of photocatalyst

The morphology and dimensions of photocatalysts were observed by field emission scanning electron microscope (FE-SEM) and images of iron doped zinc oxide composite are shown in Figure 4.6 (a) and (b). The irregular, non-uniform and highly aggregated nanoparticles are observed in ZnO nanostructure. In Figure 4.6 (a), pores of zinc oxide nanoparticles can be seen while in Figure 4.6 (b), no pores are visible and it may be because of adsorption of dye molecules onto catalyst surface during photocatalytic oxidation of dye. The chemical stoichiometric was investigated with the energy dispersive spectra (EDS). EDS spectra of Fe/ZnO (before oxidation) and iron doped ZnO (after oxidation) are shown in Figure 4.7 (a) and (b). EDS spectra of iron doped ZnO (before oxidation) reveals that sample contains three elements, Zn, Fe and O and indicates the correct doping of iron (2.5 wt%), high purity of the ZnO sample and composition. EDS spectra of iron doped ZnO (after oxidation) shows that sample contains four elements, Zn, Fe, O and C. Iron doped ZnO (after oxidation) is containing carbon due to adsorption of dye molecules onto catalyst surface during photocatalytic oxidation of dye and this results a decrease in wt% of other elements present in catalyst.

Transmission electron microscopy (TEM) image and corresponding selected-area electron diffraction (SAED) pattern of iron doped zinc oxide nanoparticles synthesized by solution combustion synthesis method is shown in Figure 4.8. For TEM analysis, sample of zinc oxide nanoparticles is prepared by dispersing iron doped zinc oxide in ethanol solution, then this solution is sonicated for about 30 min and after sonication zinc oxide nanoparticles are deposited on TEM grids coated with thin carbon or polymeric support film. From TEM image (Figure 4.8(a)), shows that all the particles are nearly spherical in shape and have an average size of 20-50 nm. This is also clear that zinc oxide nanoparticles are getting aggregated and forming a network. Figure 4.8(b) shows the selected area electron diffraction (SAED) pattern of Fe/ZnO

nanoparticles and diffraction rings shows the polycrystalline nature of iron doped zinc oxide nanoparticles. [Hamedani and Farzaneh, 2006] .

4.1.6. UV–vis spectrum studies

UV‑vis absorption spectroscopy measurements were carried out to study the changes in absorbance characteristics of dye solution during photocatalytic oxidation of dye over a range of 200-700nm. The change in absorbance characteristics of dye solution with treatment time is shown in Figure 4.9 and shows a maximum absorbance at 531 nm in the UV-vis region. The intensity of maximum absorbance peak of dye is decreasing with treatment time and this may be due to breaking of chromophore (N=N) of the dye during photocatalytic oxidation of dye. This chromophore group is responsible for color in dye solution and a decrease in the intensity of maximum absorbance peak with breaking of azo group shows that chromophore group in dye are the most active sites for oxidation attack [Shifu et al., 2011; Khorramfar et al., 2011].

4.1.7. Optical studies of iron doped zinc oxide

UV-visible diffuse reflectance spectra of the iron doped zinc oxide photocatalysts is shown in Figure 4.10. Light absorption ability of the photocatalysts can be determined with the help of UV-DRS spectra. All iron doped catalysts have maximum reflectance in UV region at 370 nm, 364 nm and 359 nm for 2.5wt% Fe/ZnO, 5wt% Fe/ZnO and 7.5wt% Fe/ZnO, whereas undoped zinc oxide is showing maximum reflectance of light at the UV-vis region at 400nm. 2.5 wt% Fe/ZnO showed maximum reflectance and reflectance decreases when dopant concentration increases. The determination of band gap of photocatalyst is very important parameter to select the right kind of light needed for the degradation of dye. Band gap energy can be calculated by using following equation [Potti and Srivastava, 2012; Tauc et al., 1970].

$$(h\nu\alpha)^{1/n} = A(h\nu - E_g) \qquad (4.1)$$

Where, h represents the Planks constant, α represents the absorption coefficient, A represents the proportional constant, ν represents the frequency of the radiation, and n has different values for different type of transition like it has a value of 0.5,1.5,2 and 3 for direct allowed transition, direct forbidden transition, indirect allowed transition and indirect forbidden transition, respectively. In this study, transition type is direct allowed transition so n has a value of 0.5 [Potti and Srivastava, 2012; Kong et al., 2009]. The acquired diffuse reflectance spectrum is

converted to Kubelka-Munk function. The α in equation () is replaced with the remission function

$$F(R_0) = (1-R_0)^2 / 2R_0 \qquad (4.2)$$

Where, R_0 represents the diffuse reflectance based on the Kubelka-Munk theory [Kong et al.,2009]. Thus equation (4.2) becomes

$$(h\nu F(R_0))^2 = A(h\nu - E_g) \qquad (4.3)$$

Band gap energy (E_g) of photocatalysts can be determined by using Tauc plot($(h\nu F(R_0))^2$ vs. $h\nu$) and are shown in Figure 4.11. Extrapolation of the linear region of the curve gives band gap energy value of photocatalysts. The estimated Band gap energy (E_g) are given in Table 4.1.

4.2. EFFECTS OF VARIOUS PARAMETERS ON PHOTOCATALYTIC DEGRADATION OF ACID RED 1 DYE

4.2.1. Effect of concentration of dopant

Now a days, ZnO is widely used photocatalyst because of its low cost, high surface reactivity with many active sites, nature of absorbing large fraction of UV spectrum than other photocatalyst. But on other hand, has several problems as fast recombination of electron hole-pair because of large band gap energy (3.37 eV), a low quantum yield in the photocatalytic reactions in aqueous solutions [Kong et al., 2009], poor utilization of visible light spectrum and photo instability because of photocorrosion under UV light and visible light [Wu et al., 2011]. In order to avoid these problems doping of transition metal ions, having similar ionic radii to zinc is done on photocatalyst so that transition metal can easily penetrate in crystal lattice of zinc oxide. Different photocatalyst were prepared by varying wt% of iron in during the synthesis of Zinc oxide and effect of transition metal doping is shown in Figure 4.12. Four types of different doping were done: 1, 2.5, 5 and 7.5wt% Fe/ZnO and their degradation efficiencies have been studied. It is shown in Figure 4.12 that the dye degradation and color removal have maximum value at 2.5 wt% Fe/ZnO. Dye degradation and color removal are increases till 2.5wt% Fe/ZnO due to availability of fewer trap sites. But for further increase in dopant concentration, degradation and color removal are decreases. This may be because of decrease in average

distance between recombination centers with increasing dopant content. By this, recombination rate increases, then the photoactivity decreases. The reduction of surface hydroxyl groups may also contributed to the low photoactivity in the presence of transition metal. Therefore, the effect of a transition metal is considered as a balance between its ability to act as an efficient trap site or as a recombination center [Wang and Egerton, 2012]. So for next experimental runs 2.5wt% Fe/ZnO photocatalyst was used.

4.2.2. Effect of calcination temperature

Calcination temperature plays a vital role in the synthesis of photocatalyst. Effect of calcination temperature on dye degradation is given Figure 4.12. Photocatalyst with different amount of iron doping were calcined at different temperature and their dye degradation and color removal ability was studied. Calcination of all photocatalysts was done 200, 400, 600, 800°C. It is clear from Figure 4.12 that for all four types of iron loading, maximum dye degradation and color removal was at 400°C. Dye degradation and color removal increased with temperature till 400°C but for higher temperature degradation and color removal decreased. Band gap energy, crystal structure, particle size and other surface properties depend upon calcination temperature [Wang et al., 2010]. Calcination temperature is also involved with the complex multi-step solid phase thermal decomposition of metal salts precursor to metal oxide [Razali et al., 2010]. Low calcination temperature leads to lower crystallization grade of photocatalyst. For achieving photocatalyst in its catalytic crystal structure, calcination temperature should be enough higher but at calcination temperatures more than 400 °C leads to the formation of larger particle size through aggregation and agglomeration. Larger particles cause loss of surface area and active sites [Wang et al., 2010; Razali et al., 2010; Zhao et al., 2012].

4.2.3. Effect of calcination time

Calcination time of photocatalyst is also a key factor as calcination temperature. Effect of calcination time on dye degradation and color removal is given in Figure 4.13. Calcination time was varied from 1 to 5 hr while calcination temperature was kept constant (400°C). Here, it is clear from the Figure 4.13 that dye degradation and color removal increased with an increase calcination time till 4 h but after 4 h, dye degradation and color removal started decreasing. Low calcination time results is low crystal size of catalyst. From Figure 4.13, it can be seen that dye degradation and color removal is increasing with calcination time and this may be because of increase in crystal size of catalyst [Reli et al, 2012]. After an optimum duration of calcination,

degradation and color removal decrease because of probable occurrence of conglomeration of photocatalyst [Wang et al., 2009].

4.2.4. Effect of catalyst dosage

The effect of catalyst loading on color removal and degradation of azo dye by photocatalytic oxidation process under UV light is shown in Figure 4.14. Photocatalytic oxidation of acid red 1 is done at three different type of catalyst loading: 1, 1.25 and 1.5 g/L while other parameters were kept constant. It is clear from Figure 4.14 that as catalyst loading increases, dye degradation and color removal also increase. Maximum dye removal (≈99%) and color removal(73%) are at catalyst loading of 1.5 g/L but at catalyst loading of 1.25 g/L, dye degradation(94%) and color removal(71%) are not much less than 1.5g/L so from fig 4.8.it can be observed that optimum catalyst loading for photocatalytic degradation of acid red 1 dye under UV light is 1.25 g/L. Increase in dye degradation by increasing catalyst loading may be caused by increase in number of active sites present on photocatalyst for dye degradation and penetration of radiation through the suspension [Jamil et al., 2012]. Optimum catalyst dosage of 1.25g/L was used for subsequent studies of azo dye degradation.

4.2.5. Effect of pH of dye

pH of the solution plays a key role in degradation of dye**.** Hydroxyl radical concentration, charge of the molecule, adsorption of dye molecule onto photocatalyst surface and Surface charge property of the photocatalyst depend upon pH of dye solution [Jamil et al., 2012]. pH of solution was varied from 2 to 11 to study its effect on the photocatalytic degradation of the acid red 1 dye and shown in Figure 4.15(a). It can be observed from Figure 4.15 (a). that at low pH (2-3) dye degradation and color removal is maximum and as pH tending to basic, degradation and color removal are decreasing. It may be because of high rate of adsorption of dye onto catalyst surface at low pH and it is decreasing as pH is increasing. ZPC (Zero point charge) of the ZnO has a value ≈ 10.0 and catalyst surface is positively charged below point of zero charge and negatively charged above the point of zero charge as shown in Figure 4.15 (b) [Akyol and Bayramoglu, 2005; Sobana and Swaminathan, 2007; Lu et al., 2009; Wang et al., 2010; Hasnat et al., 2007] and acid red 1 dye has pK_a values of 7.5 for azonium group and 10.0 for naphtholic group [Bicer and Arat, 2009]. In aqueous solution, sulphonate groups (D-SO_3Na) of dye are dissociated and convert the dye in anionic dye ions ($D-SO_3^-$). It is clear from these factors that at low pH, strong attractive forces between dye molecules and the catalyst surface will give high

rate of adsorption of dye onto catalyst surface and high degradation and color removal value as well.

4.2.6. Effect of oxidant dosage

The effect of oxidant dosage on color removal and degradation of azo dye by photocatalytic oxidation process under UV light is shown in Figure 4.16. To optimize oxidant dosage, it was varied from 3 to 10 m mol/L. It can be seen from Figure 4.16 that dye degradation and color removal are increasing with oxidant dosage upto 6 mol/L, due to increase in the formation of $OH^{\cdot}$ Radicals[Tekbas et al., 2008]. Further increase in oxidant dosage gives a reduction in dye degradation and color removal. This reduction in dye degradation and color removal is may be due to occurrence of self scavenging of $OH^{\cdot}$ Radicals and also gives a lower utilization of H_2O_2.[Lucas and Peres, 2006]. Scavenging effect lowers the concentration of $OH^{\cdot}$ Radicals and can be expressed by the eq. (4.1). So it can be said from fig. that 6 mmol/L is an optimum dosage for Acid red 1 dye degradation because it produces enough hydroxyl radicals for photocatalytic oxidation of dye.

$$HO_2^{\cdot} + HO^{\cdot} \rightarrow H_2O + O_2 \qquad (4.1)$$

4.2.7. Effect of reaction temperature

The reaction temperature is very important parameter in photocatalytic process because it controls the formation of hydroxyl radicals during the reaction. The catalyst iron doped ZnO was tested at three temperatures: 30°C, 40°C and 50°C and results are shown in Figure 4.17 It is clear from the Figure 4.17 that degradation of dye and color removal of dye is increasing by increasing temperature from 30°C to 50°C. An increase in temperature results accelerated reaction rate between H_2O_2 and the catalyst and enhances the rate of formation of hydroxyl radicals. Hydroxyl radicals having high oxidizing potential oxidize organic matter present in wastewater into CO_2 and H_2.

4.2.8. Effect of initial concentration of dye

The effect of initial dye concentration on dye degradation and color removal is shown in Figure 4.18. Initial dye concentration was varied from 25 mg/L to 100 mg/L while other experimental variables were kept constant. Degradation of dye increases by increasing initial concentration of dye upto 50 mg/L. At initial dye concentration of 50 mg/L, dye degradation and color removal values are higher because of presence of enough dye molecules in comparison to

$OH^{\cdot}$ radicals for the degradation of dye. For dye concentration of 25 mg/L, dye degradation and color removal are lower than that of 50 mg/L and this may be because of less no. of dye molecules present in solution and lower utilization of $OH^{\cdot}$ radicals [Lucas and Peres, 2006]. A decrease can be observed from fig. in dye degradation and color removal from 50 mg/L to 100 mg/L because the increase in dye concentration increases the dye molecules present in solution and also increases the competition with $OH^{\cdot}$ radicals [Tekbas et al.,2008]. Penetration of light through photocatalyst can be another reason for decrease in dye degradation by increasing initial dye concentration due to adsorption of dye molecules on photocatalyst surface. At high concentration of dye, dye molecules adsorbed on catalyst surface can absorb UV light rather than photocatalyst and this affects the activity of photocatalyst [Jamil et al.,2012].

4.2.9. Effect of reaction time

In order to determine the reaction kinetics of photocatalytic degradation, the relationship between concentration (C) and reaction time (t) is plotted as shown in Figure 4.19. It is found that the degradation reaction of acid red 1 dye basically obeys the pseudo first-order reaction kinetics. The rate constant was calculated from the plot of the natural logarithm of the dye concentration as a function of irradiation time. The rate constant (k) is 0.01195 min^{-1} for 2.5 wt% Fe/ZnO and R^2 (goodness of fit) value is 0.98. it may be seen in Figure 4.19 that the zeta potential of the dye solution increased from negative value during initial phases of the treatment.

pK_a values for azonium group is 7.5 and for naphtholic group is 10.0 [Bicer and Arat, 2009], therefore it is positively charged at pH 7 and the solution has a negative potential. With degradation, azo bonds breaks and the zeta potential value becomes positive as seen in the Figure 4.19.

Table 4.1 Physico-chemical characteristics of Catalysts

Characteristics	**2.5wt% Fe/ZnO**
Surface area of pores (m^2/g)	
(i) BET	64.5150
(ii) BJH	
(a) adsorption cumulative	70.816
(b) desorption cumulative	80.3583
BJH cumulative pore volume (cm^3/g)	
(i) Single Point Total	0.119049
(ii) BJH adsorption	0.117620
(iii) BJH desorption	0.119964
Average pore diameter (Å)	
(i) BET	73.8120
(ii) BJH adsorption	66.437
(iii) BJH desorption	59.714

Table 4.2 Structural and crystallographic characteristics of both ZnO and Fe/ZnO catalyst

Undoped ZnO				
Rel. Int. [%]	**d-spacing [Å]**	**Pos. [°2Th.]**	**FWHM [°2Th.]**	**Tip width [°2Th.]**
100	2.48936	36.0506	0.456	0.38
64.56	2.83132	31.5742	0.3192	0.266
54.59	2.81802	31.7272	0.1824	0.152
49.14	2.62285	34.1578	0.228	0.19
28.4	1.62667	56.5293	0.2052	0.171
27.64	1.63491	56.219	0.2052	0.171
25.52	17.44872	5.0605	0.1824	0.152
22.62	1.48414	62.5332	0.228	0.19
20.35	1.38355	67.6634	0.1824	0.152
18.42	15.99929	5.5192	0.1824	0.152
18.02	1.37898	67.9185	0.2736	0.228
17.42	1.92408	47.1998	0.1824	0.152
16.62	1.91551	47.4239	0.1596	0.133
11.5	1.36093	68.9448	0.2052	0.171
10.88	1.47202	63.1072	0.2052	0.171
2.5wt%Fe/ZnO				
Rel. Int. [%]	**d-spacing [Å]**	**Pos. [°2Th.]**	**FWHM [°2Th.]**	**Tip width [°2Th.]**
100	2.47682	36.2395	1.0944	0.912
70.83	17.1591	5.1459	0.228	0.19
66.72	2.81688	31.7404	0.3648	0.304
50.09	2.61568	34.2543	0.456	0.38
49.59	15.99055	5.5223	0.1824	0.152
36.54	1.6292	56.4334	0.1824	0.152
20.4	1.47935	62.7585	0.2052	0.171
17.84	1.3642	68.7563	0.2052	0.171
16.64	1.3922	67.1871	0.1824	0.152
13.93	2.38558	37.6766	0.1596	0.133
10.98	1.89769	47.8969	0.5472	0.456
5.51	1.5099	61.3496	0.3648	0.304
4.34	1.09745	89.1595	0.456	0.38
4.3	1.43907	64.7252	0.1824	0.152
4.2	1.2372	77.0149	0.1824	0.152

Table 4.3 Band gap energies of iron doped zinc oxide photocatalysts

Catalyst	Band gap energy (E_g)
Undoped ZnO	3.38
1wt% Fe/ZnO	-
2.5wt% Fe/ZnO	3.14
5wt% Fe/ZnO	3.19
7.5wt% Fe/ZnO	3.24

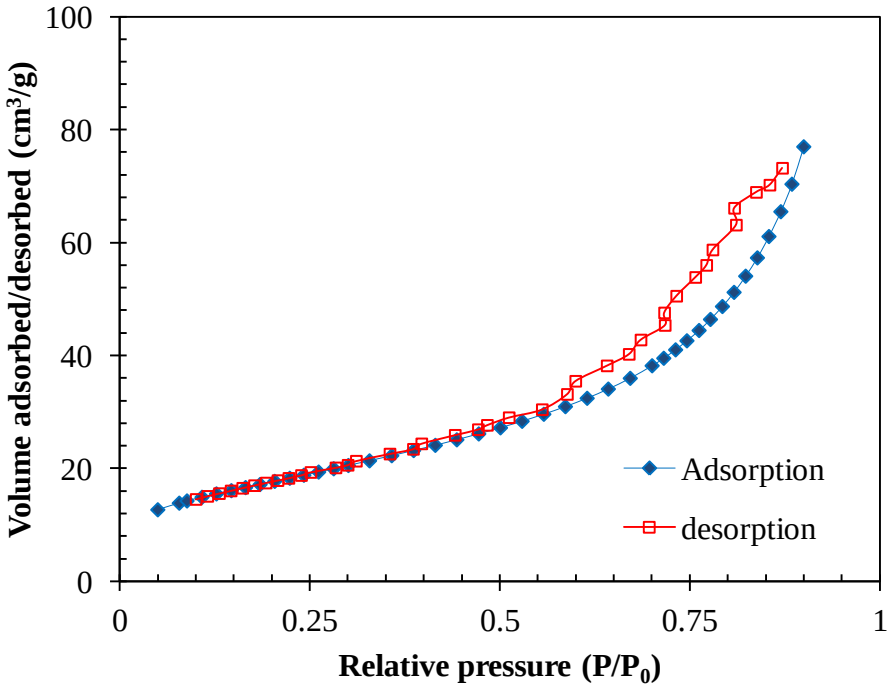

Figure 4.1 Adsorption/desorption isotherms of N_2 at 77K on Fe/ZnO.

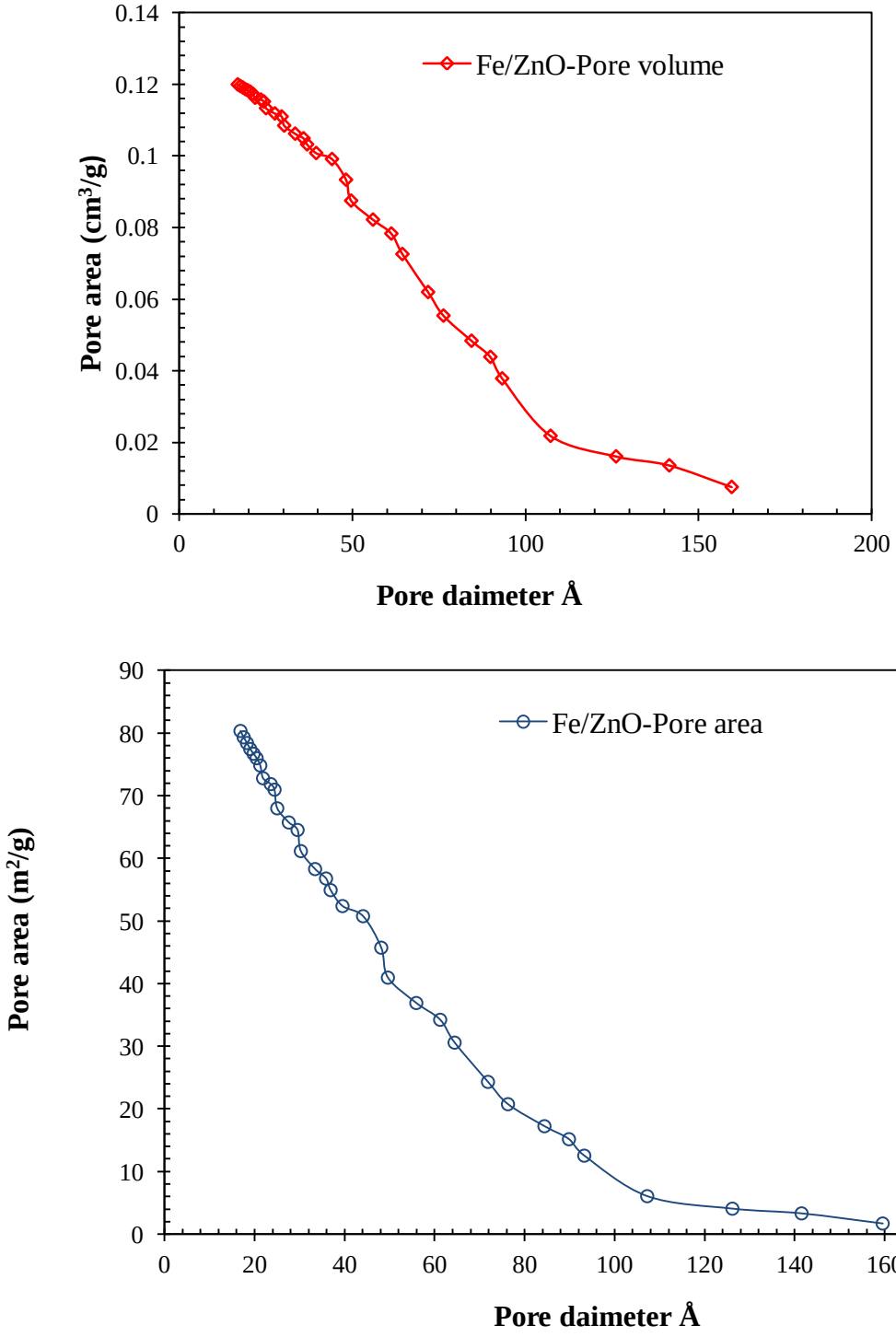

Figure 4.2 Pore size distribution of 2.5wt% Fe/ZnO

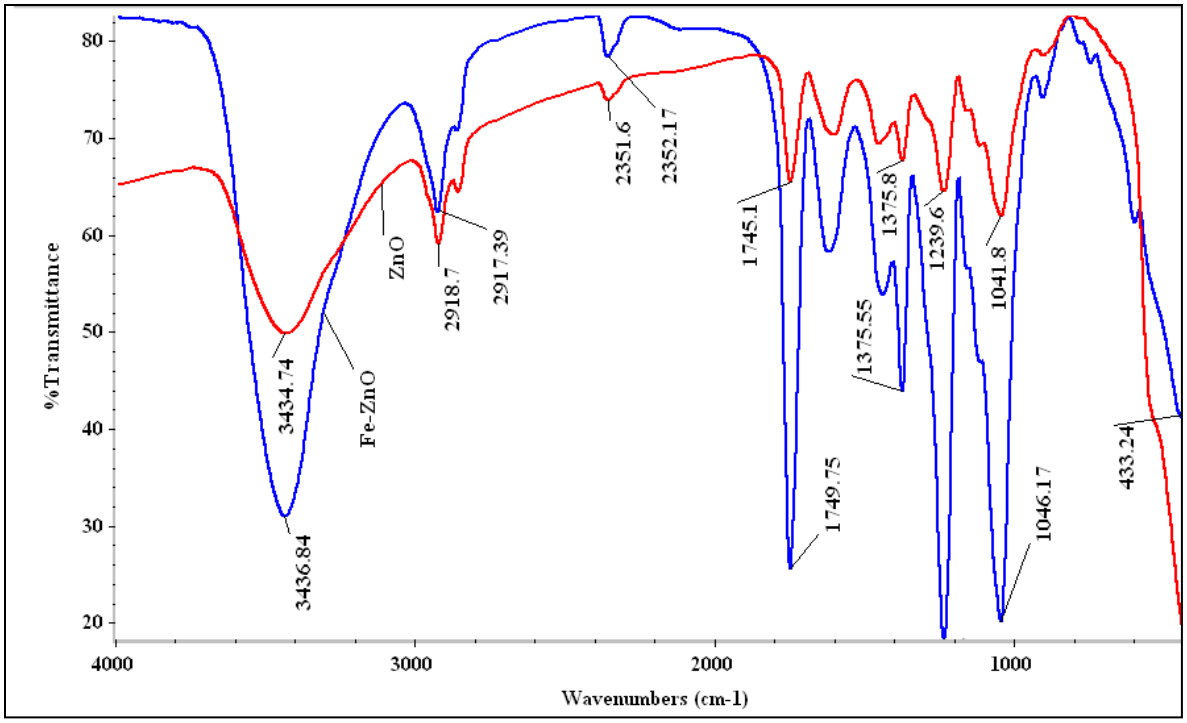

(a)

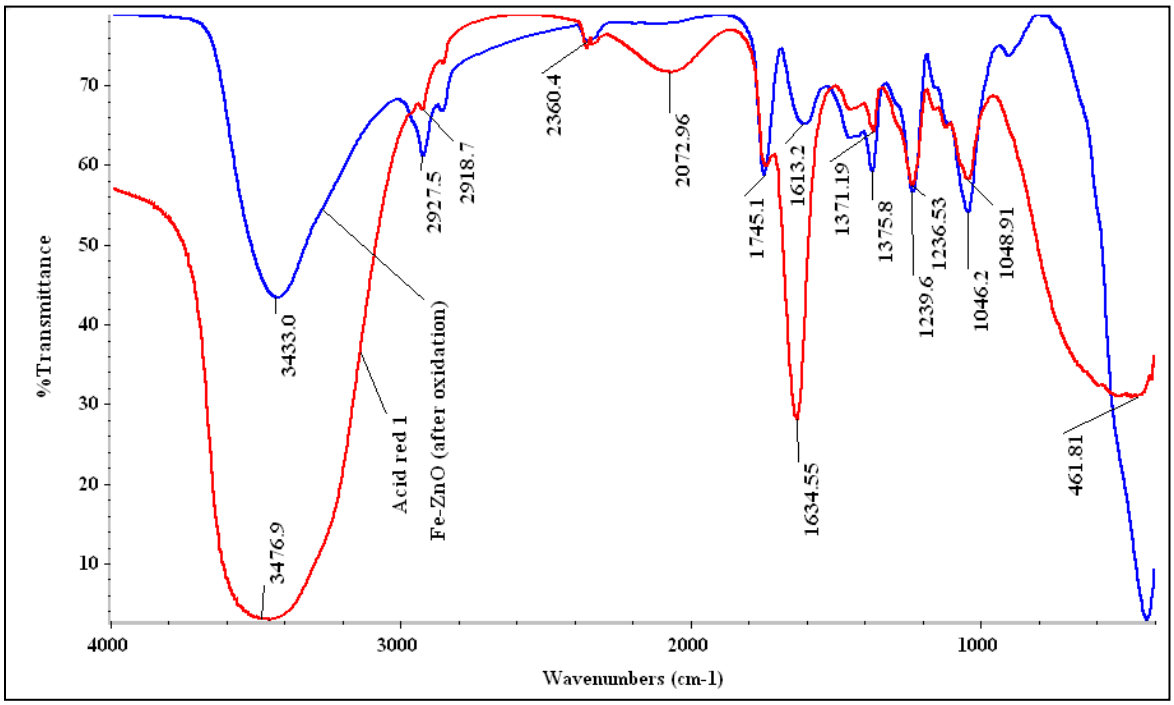

(b)

Figure 4.3 FTIR spectra of (a) undoped and 2.5wt% iron doped ZnO, (b) Acid red 1 dye and 2.5wt% Fe/ZnO (after oxidation).

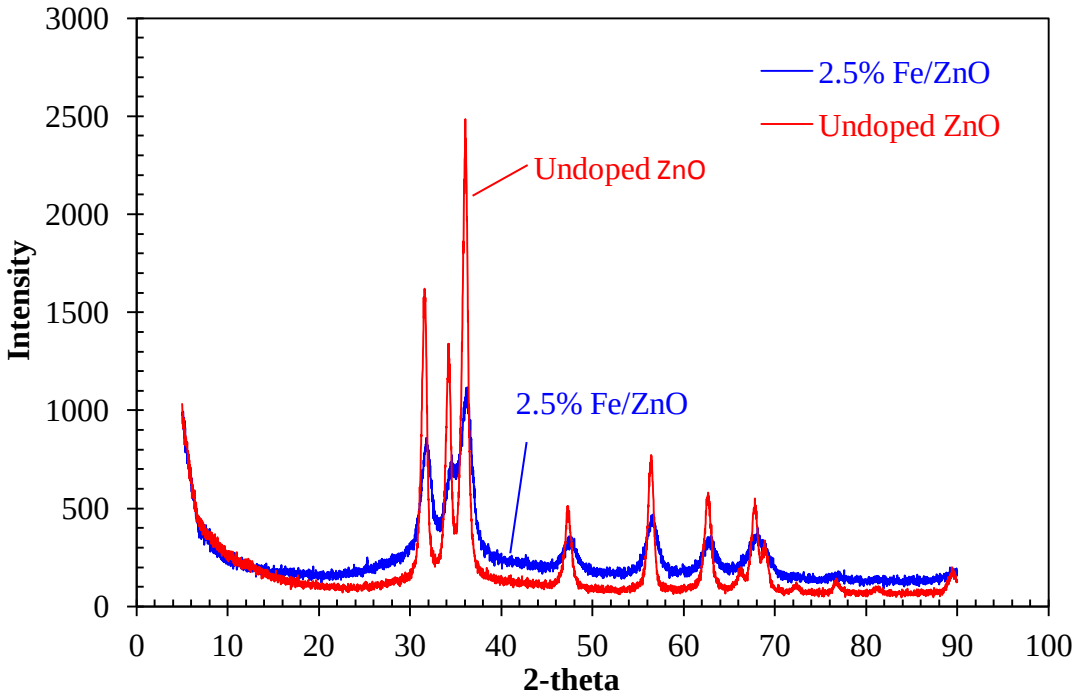

Figure 4.4 XRD patterns of undoped ZnO and 2.5wt% iron doped ZnO.

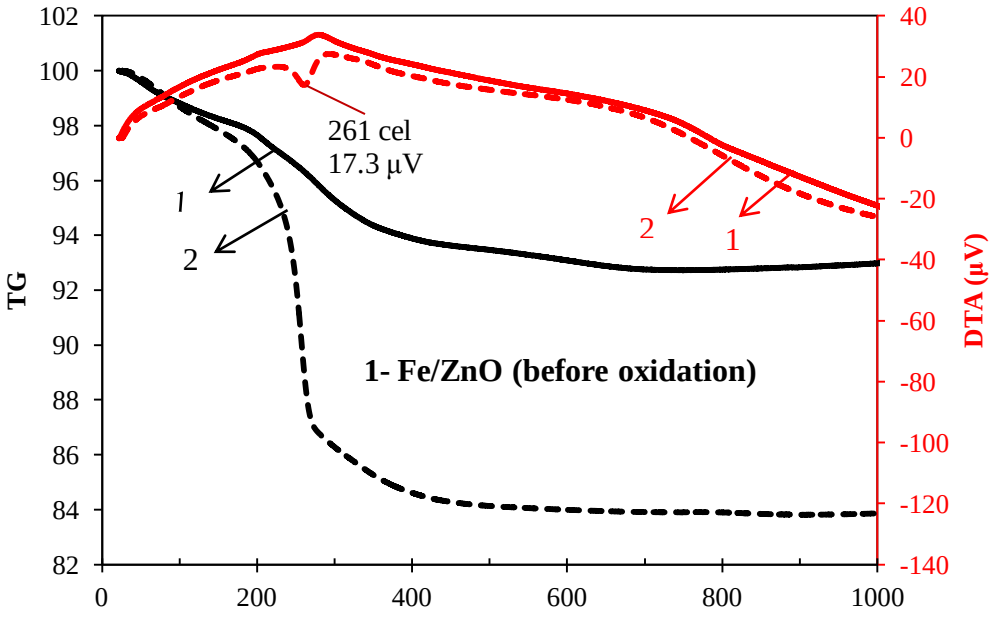

Figure 4.5 Differential thermal gravimetric analysis and differential thermal analysis of 2.5wt% Fe/ZnO.

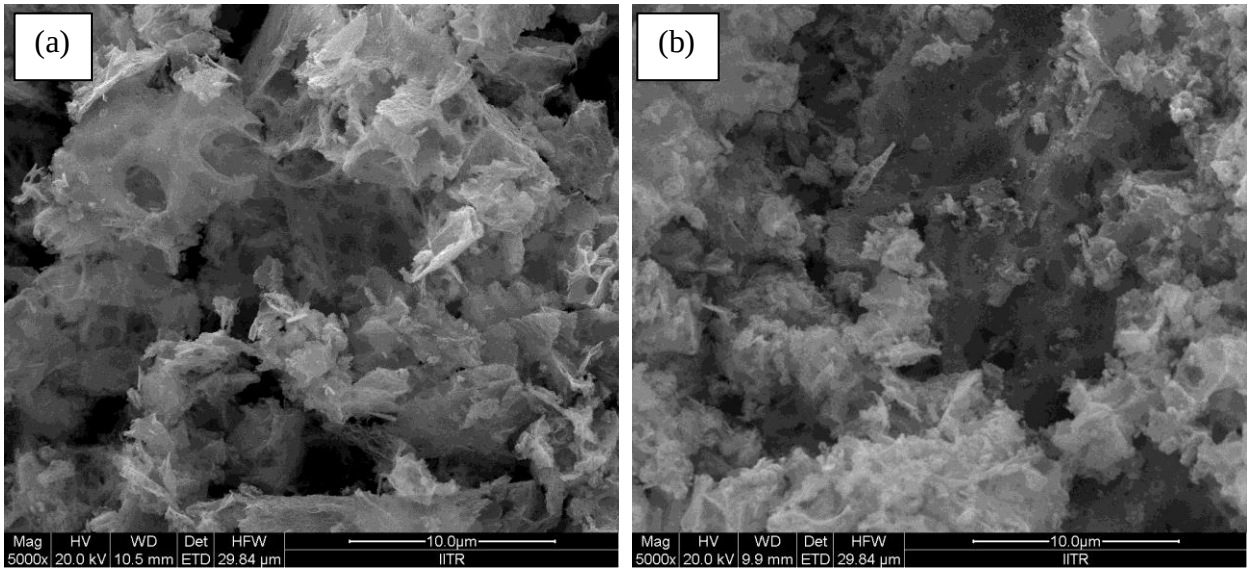

Figure 4.6 FE-SEM images of 2.5wt% Fe/ZnO (a) before oxidation, (b) after oxidation.

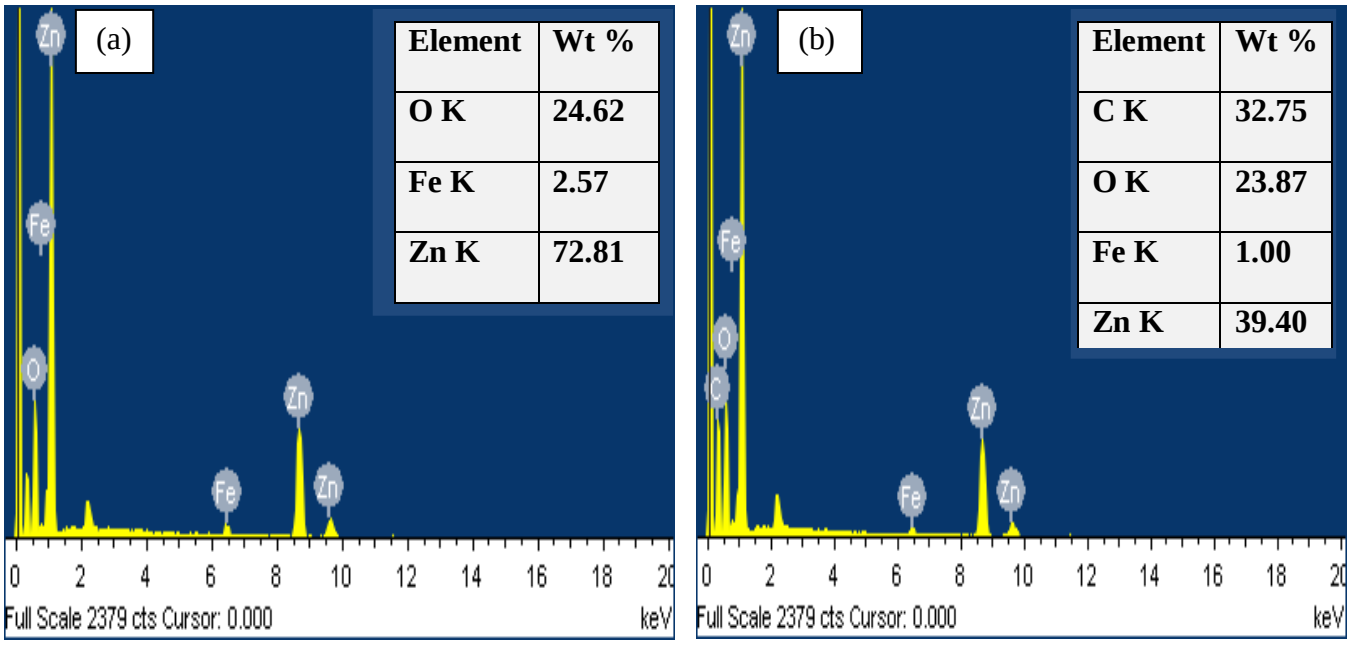

Figure 4.7 EDS patterns of 2.5wt% Fe/ZnO (a) before oxidation, (b) after oxidation.

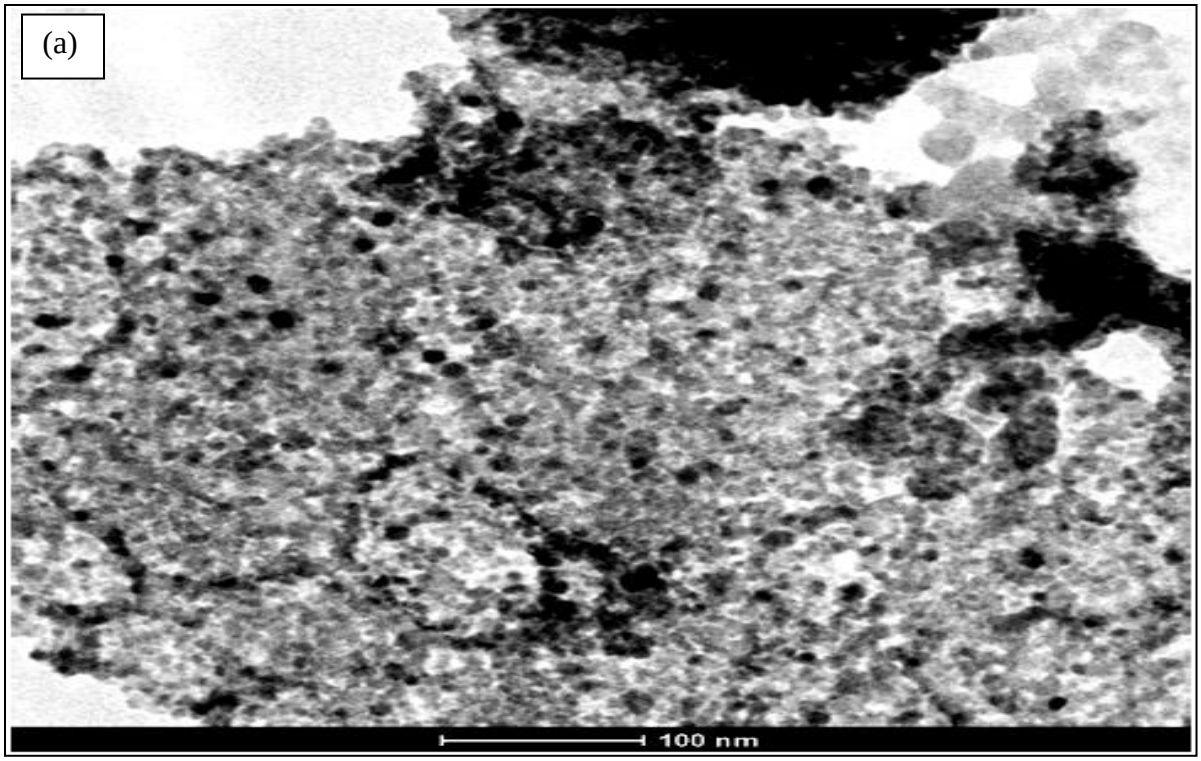

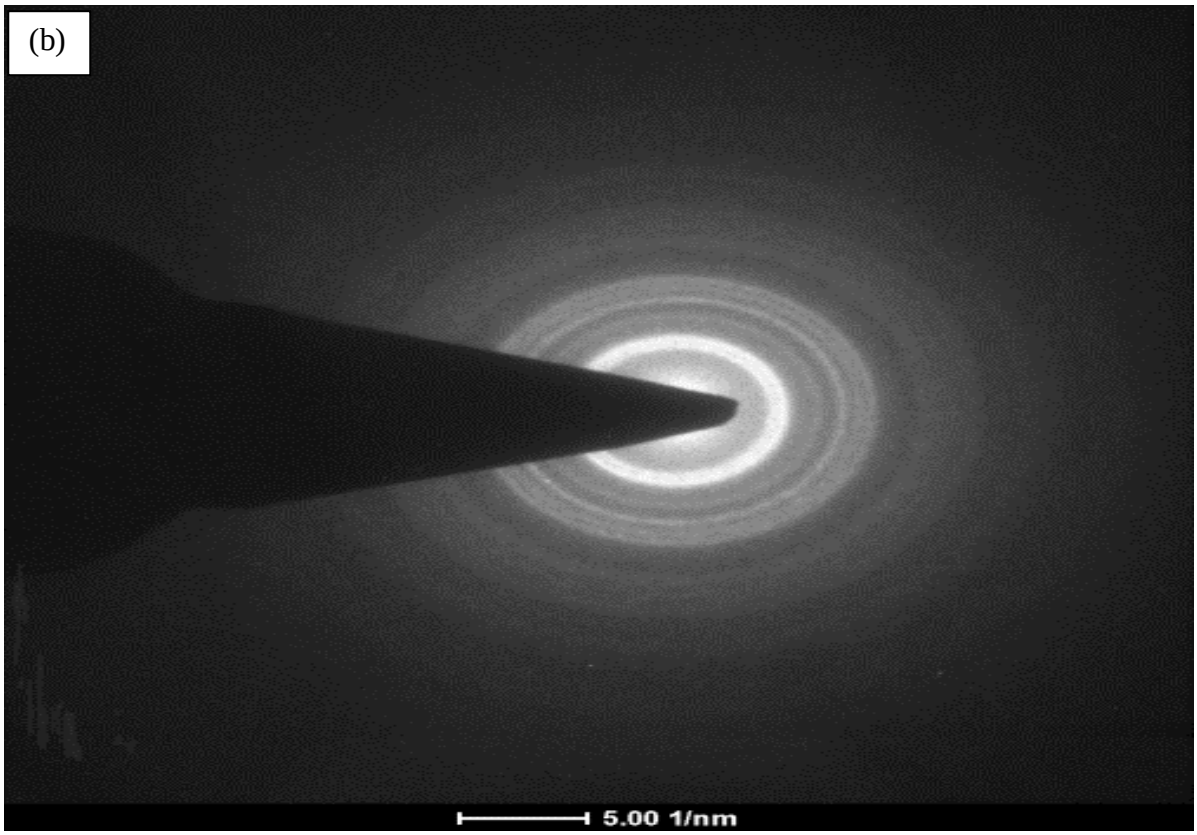

Figure 4.8(a) TEM images and (b) SAED patterns of 2.5wt% Fe/ZnO.

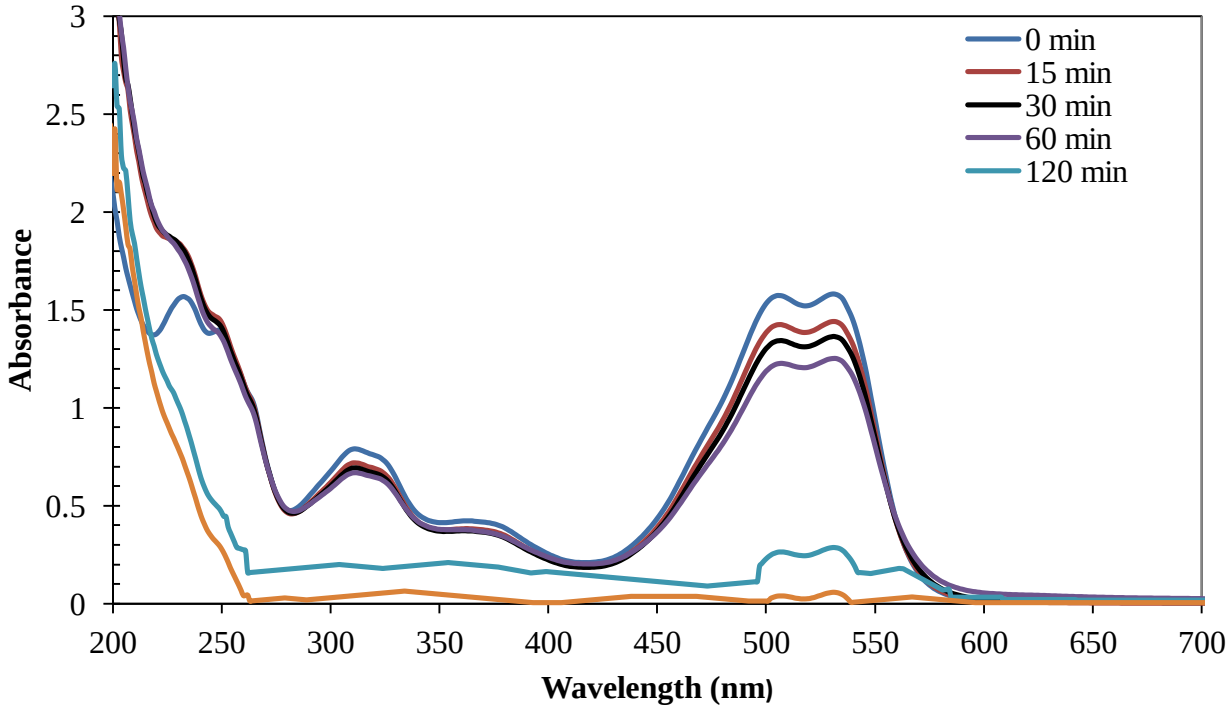

Figure 4.9 Changes in the UV-vis absorption spectra of acid red 1 dye with reaction time.

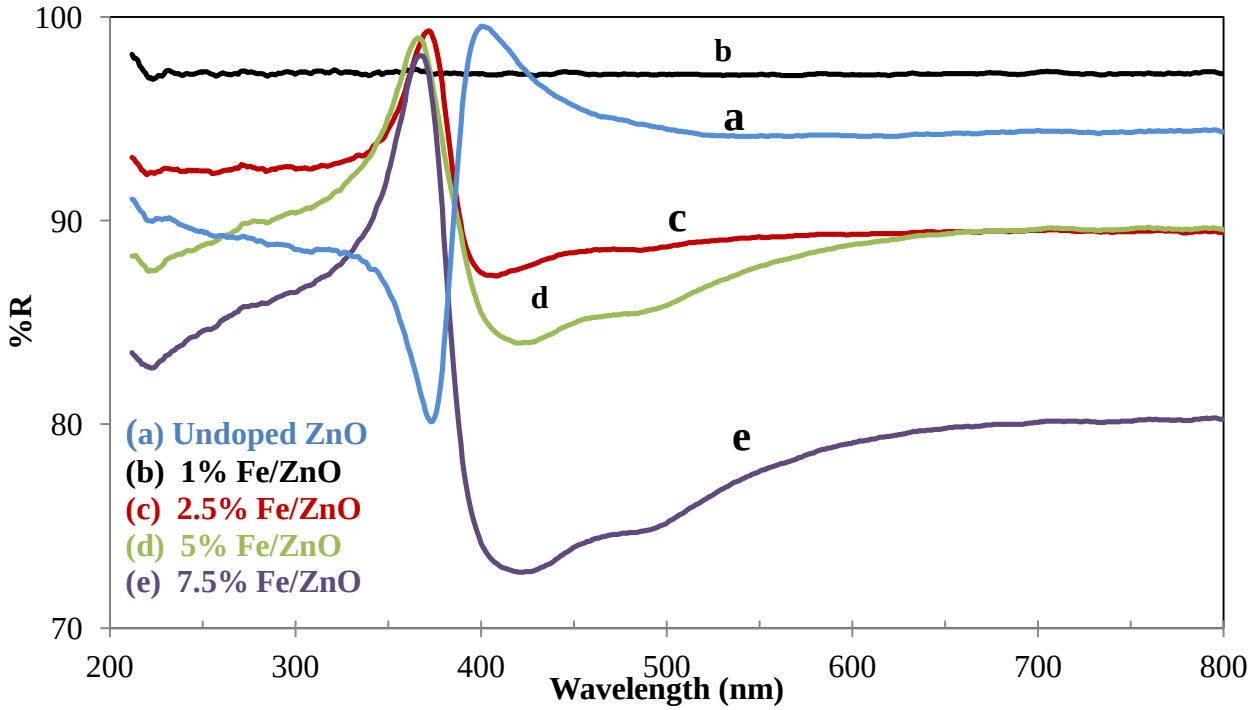

Figure 4.10 DRS spectra of iron doped ZnO particles.

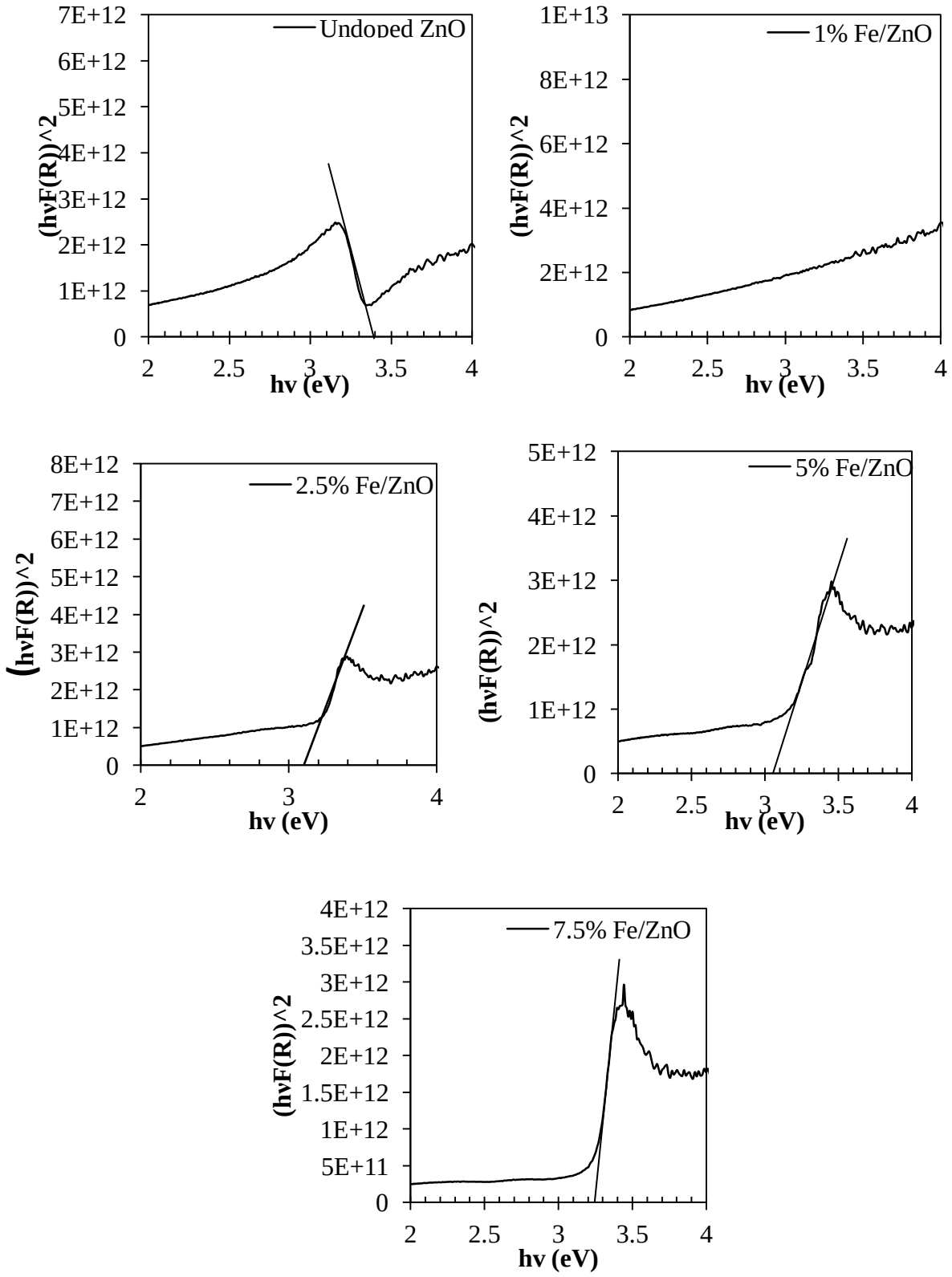

Figure 4.11 Tauc plots of the undoped and iron doped samples.

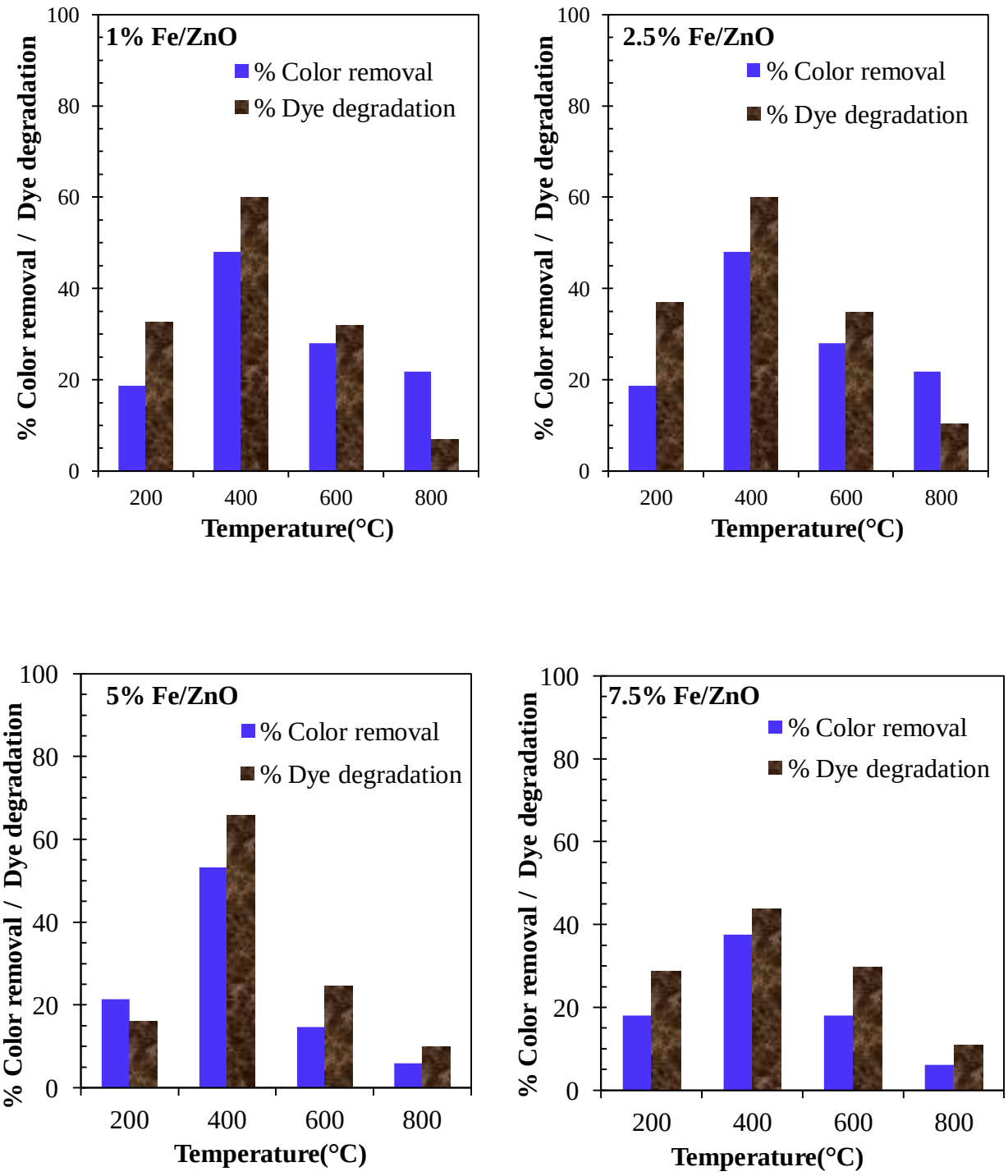

Figure 4.12 Effect of concentration of dopant and calcination temperature on dye degradation and color removal of acid red 1 dye. (Calcination time= 4 h, Initial dye concentration= 50 mg/l, Initial color = 2730 Pt:Co, catalyst dosage= 1g/l, Oxidant dosage=60.45 m/m)

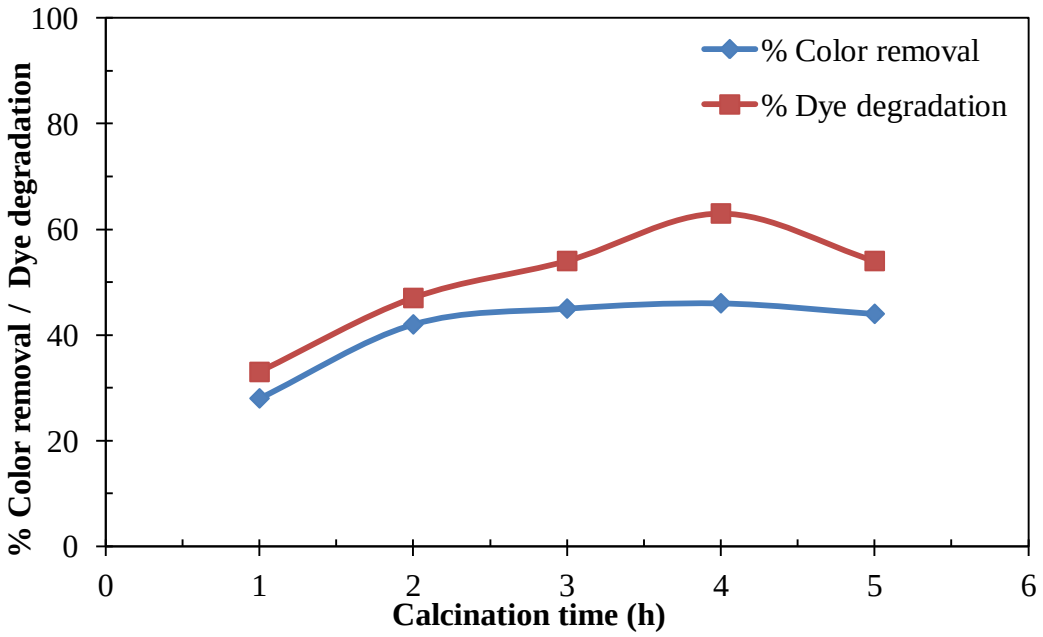

Figure 4.13 Effect of calcination time on dye degradation and color removal of acid red 1 dye (Catalyst =2.5% Fe/ZnO, Calcination temp.= 400°C, Initial dye conc.= 50 mg/l, Initial color= 2730 Pt:Co, catalyst dosage= 1 g/l, Oxidant dosage=60.45 m/m).

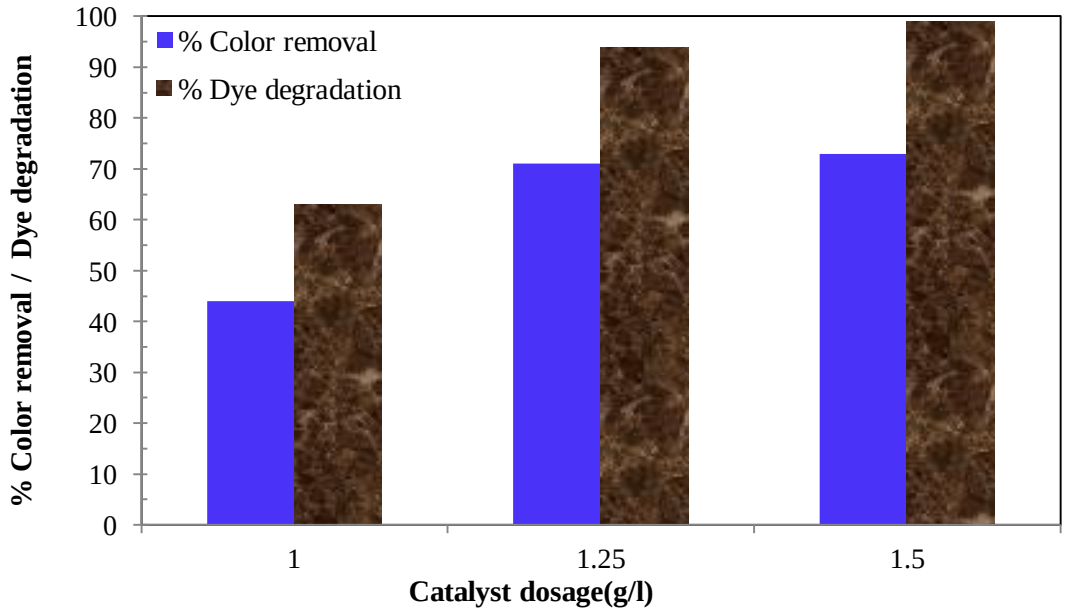

Figure 4.14 Effect of photocatalyst dosage on color removal and dye degradation (Catalyst =2.5% Fe/ZnO, Calcination temperature= 400°C, Calcination time= 4 h, Initial dye conc= 50 mg/l, Initial color= 2730 Pt:Co, Oxidant dosage=60.45 m/m).

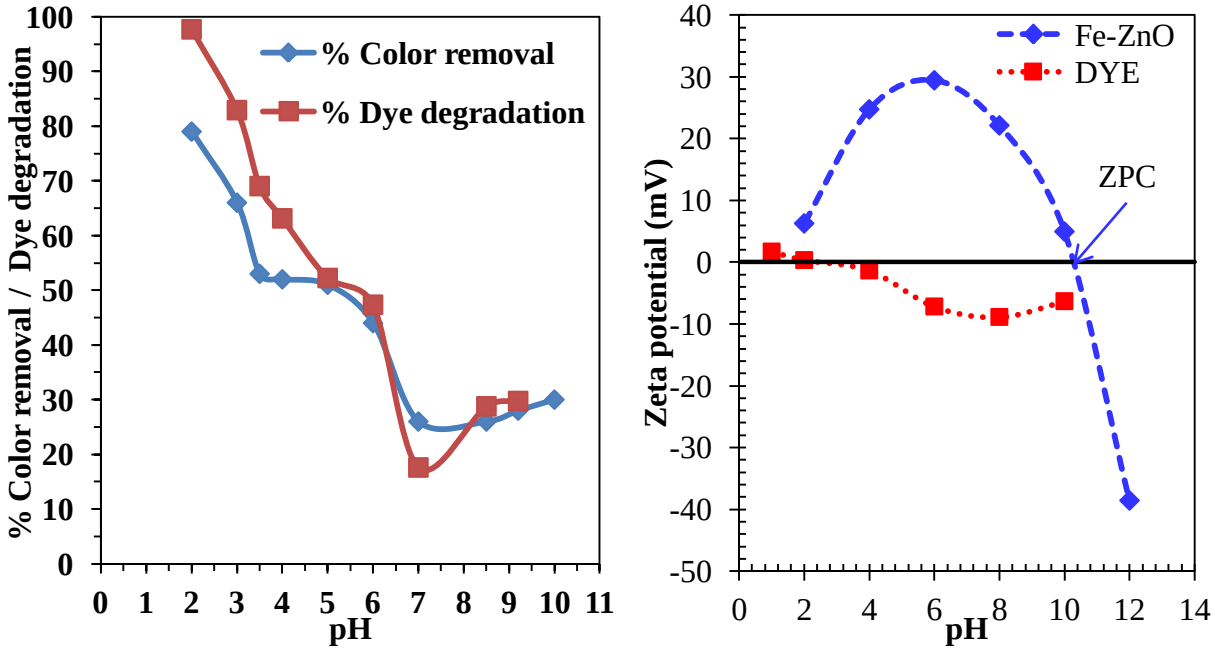

Figure 4.15 (a) Effect of pH of dye solution, (b) zeta potential of acid red 1 dye on dye degradation, color removal (Catalyst =2.5%Fe/ZnO, Calcination temp.= 400°C, Calcination time= 4 h, Initial dye conc.= 50 mg/l, Initial color= 2730 Pt:Co, catalyst dosage= 1.25 g/l, Oxidant dosage=60.45 m/m).

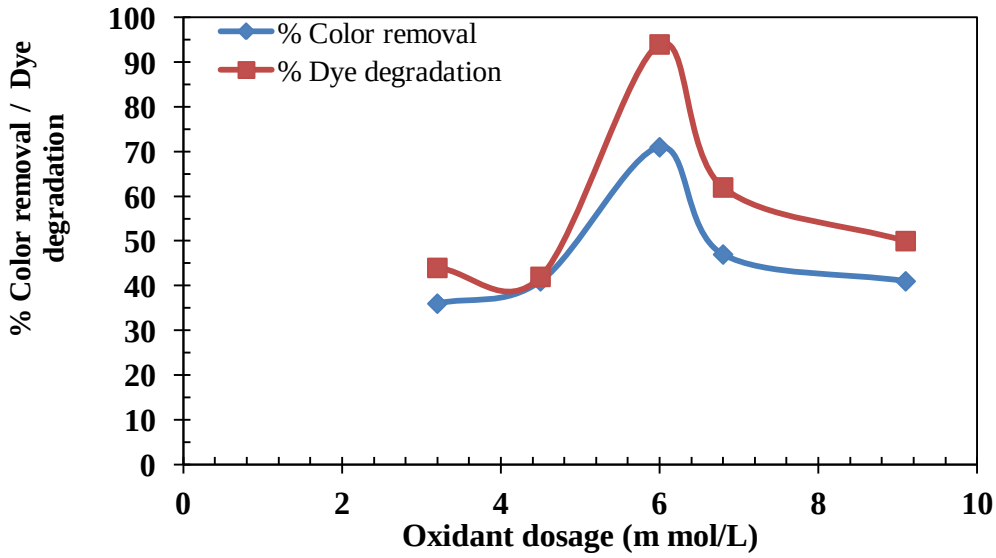

Figure 4.16 Effect of Oxidant dosage on color removal and dye degradation (Catalyst =2.5% Fe/ZnO, Calcination temperature= 400°C, Calcination time= 4 h, Initial dye conc.= 50 mg/l, Initial color= 2730 Pt:Co, Catalyst dosage=1.25 g/l).

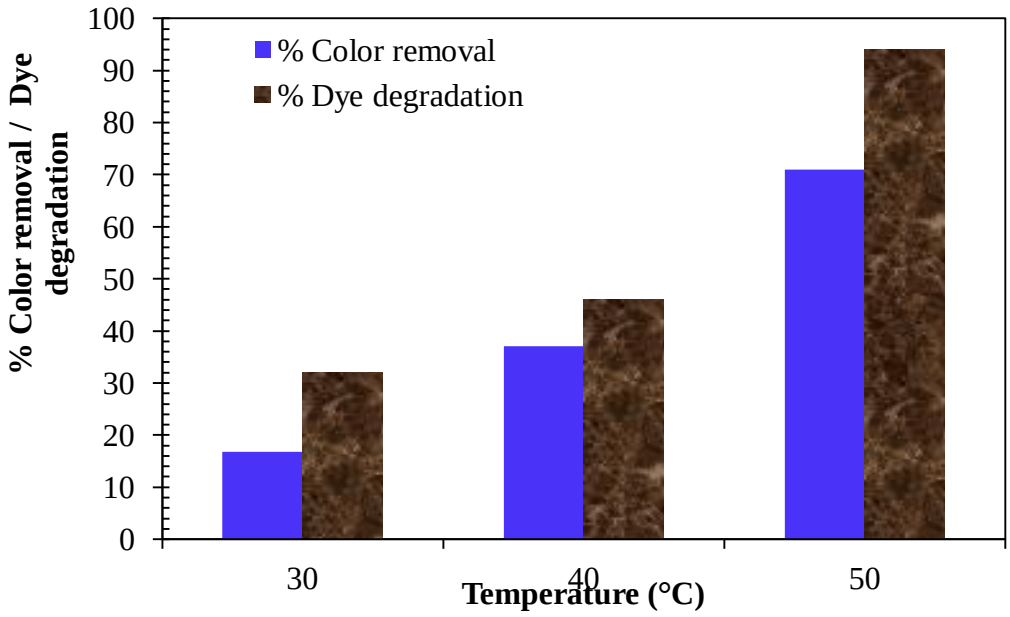

Figure 4.17 Effect of Reaction temperature on color removal and dye degradation (Catalyst =2.5% Fe/ZnO, Calcination temp.= 400°C, Calcination time= 4 h, Initial dye conc.= 50 mg/l, Initial color= 2730 Pt:Co, Catalyst dosage=1.25 g/l, oxidant dosage= 6 m mol/l).

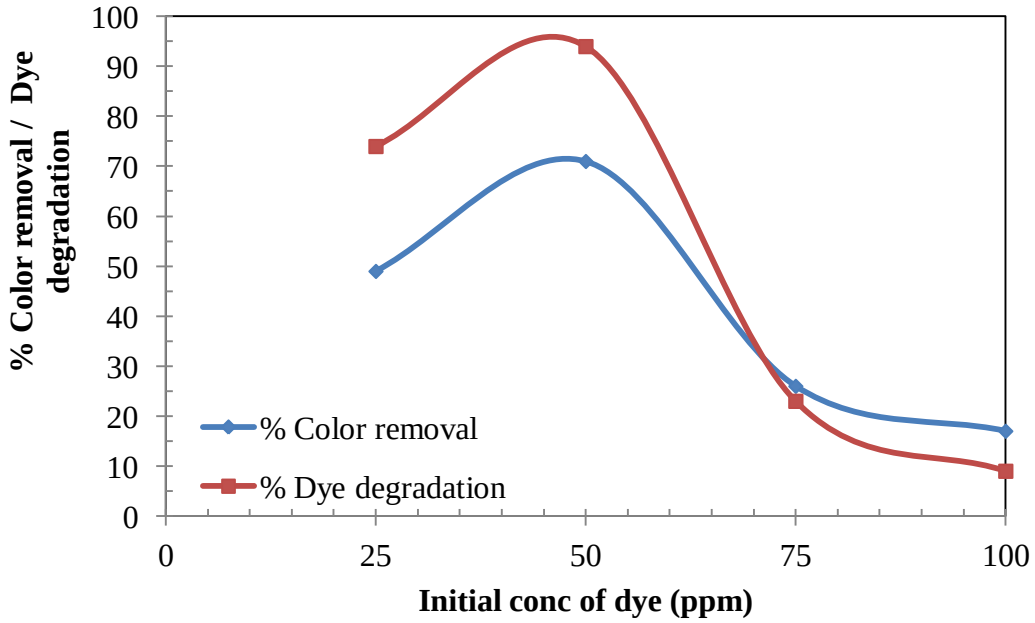

Figure 4.18 Effect of Initial concentration of dye on color removal and dye degradation (Catalyst =2.5% Fe/ZnO, Calcination temp= 400°C, Calcination time= 4 h, Initial dye conc.= 50 mg/l, Initial color= 2730 Pt:Co, Catalyst dosage=1.25 g/l, oxidant dosage= 6 m mol/l).

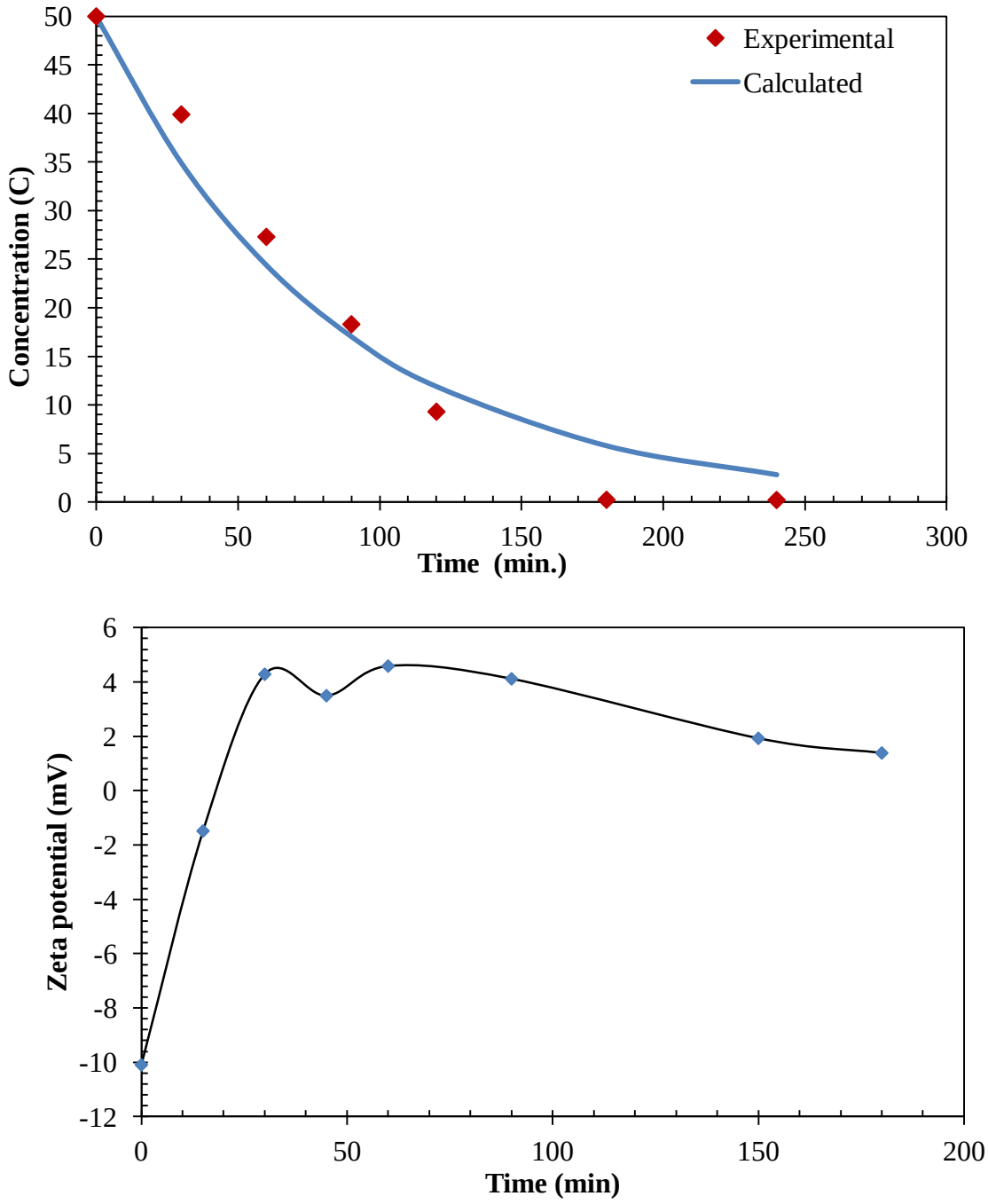

Figure 4.19 Time dependence of concentration and zeta potential of acid red 1 dye (Catalyst =2.5% Fe/ZnO, Calcination temp. = 400°C, Calcination time= 4 h, Initial dye conc.= 50 mg/l, Initial color= 2730 Pt:Co, pH≈7, catalyst dosage= 1.25 g/l, Oxidant dosage=6 m mol/l.

5. CONCLUSION AND RECOMMENDATIONS

5.1. CONCLUSIONS

The present study aimed to synthesize, characterize and use iron doped zinc oxide (Fe/ZnO) as a photocatalyst for use in oxidative treatment of acid red 1 dye bearing wastewater. On the basis of the studies performed and the results and discussions presented earlier, the following conclusions can be made:

1. Various iron doped ZnO catalysts have been synthesized using solution combustion synthesis method (SCS). This method is very fast and effective to prepare photocatalyst with high crystal grade.
2. BET surface area analysis of 2.5wt% Fe/ZnO indicated a mixture of micro-porous and mesoporous material and have BET surface area and pore diameter of 64.51 m^2/g and 73.81 Å.
3. XRD analysis confirmed that ZnO and Fe/ZnO have standard hexagonal wurtzite structure, but doping of iron decreases the crystallinity of ZnO.
4. FE-SEM and EDS analysis of 2.5wt% Fe/ZnO and 2.5wt% Fe/ZnO (after oxidation) showed irregular, non-uniform and highly aggregated nanoparticles and adsorption of dye molecules onto the surface of catalyst after oxidation.
5. UV-DRS analysis of undoped and all doped catalysts showed no impurity phase, undoped ZnO showed maximum reflectance intensity in UV-vis region and all doped samples showed maximum reflectance intensity in UV region except 1wt% Fe/ZnO. Bang gap energy (e_g) of all samples are in the range of 3.38-3.14 eV.
6. Photocatalytic activity of iron doped zinc oxide have been tested by photocatalytic oxidation of acid red 1 dye and the effects of preparatory conditions and operational parameters on the photocatalytic oxidation of acid red 1 dye were studied.
7. Optimum conditions for photocatalytic oxidation of acid red 1dye were found as: iron doping=2.5wt%, calcination temperature=400℃, calcination time=4 h, catalyst dosage=1.25 g/l, pH ≈2.0, oxidant dosage= 6 mmol/l and reaction temperature= 50°C.

5.2. RECOMMENDATIONS

On the basis of the present studies, the following recommendations can be made for future studies:

1. Different photocatalytic oxidation trials of acid red 1 dye may be done under solar light irradiation.
2. Fe/ZnO catalysts can be synthesized using other synthesis methods and their photocatalytic degradability can be tested.

REFERENCES

Akyol A. and Bayramoglu M., "Photocatalytic degradation of Remazol Red F3B using ZnO catalyst", Journal of Hazardous Materials B124 (2005) 241–246.

Ali R., Azelee W., Bakar W. A. & Teck L. K., "Zn/ZnO/TiO_2 and Al/Al_2O_3/TiO_2 Photo catalysts for the Degradation of Cypermethrin", Modern applied science, Vol.4 (2010) No. 1.

Asilturk M., Sayılkan F., Arpac E., "Effect of Fe^{3+} ion doping to TiO_2 on the photocatalytic degradation of Malachite Green dye under UV and vis-irradiation", Journal of Photochemistry and Photobiology A: Chemistry 203 (2009) 64‑71.

Barick K.C., Singh S., Aslam M., Bahadur D., "Porosity and photocatalytic studies of transition metal doped ZnO nanoclusters", Microporous and Mesoporous Materials 134 (2010) 195–202.

Biçer E. and Arat C., "A Voltammetric Study on the Aqueous Electrochemistry of Acid Red 1 (Azophloxine)", Croat. Chem. Acta 82 (3) (2009) 583–593.CCA-3349.

Carliell C.M., Barclay S.J., Buckley C.A., "Microbial decolourization of a reactive azo dye under anaerobic conditions", Water Research Commission South Africa, 1995, pp. 61–69.

Chacon J. M., Leal M.T., Sanchez M., Banda E. R. "Solar photocatalytic degradation of azo-dyes by photo-Fenton process", Journal of Dyes and Pigments 69(2006) 144-150.

Chakrabarti S., Dutta B.K., "Photocatalytic degradation of model textile dyes in wastewater using ZnO as semiconductor catalyst", Journal of Hazardous Materials B,112,269-278.

Changlin Y.U., Kai Y., Qing S., Jimmy Y.U., Fangfang C., Xin L., "Preparation of WO3/ZnO Composite Photocatalyst and Its Photocatalytic Performance", CHINESE JOURNAL OF CATALYSIS; Volume 32 (2011) Issue 4.

Chen K.J., Fang T.H., Hung F.Y., Ji L.W., Chang S.J., Young S.J., Hsiao Y.J., "The crystallization and physical properties of Al-doped ZnO nanoparticles", Applied Surface Science 254 (2008) 5791‑5795.

Chen T., Zheng Y., Lin J.M., Chen G., "Study on the Photocatalytic Degradation of Methyl Orange in Water Using Ag/ZnO as Catalyst by Liquid Chromatography Electrospray Ionization Ion-Trap Mass Spectrometry", J Am Soc Mass Spectrom 19 (2008) 997–1003.

E. Kusvuran, O. Gulnaz, S. Irmak, O.M. Atanur, H.I. Yavuz, O. Erbatur, Comparison of several advanced oxidation processes for the degradation of reactive red 120 azo dye in aqueous solution, J. Hazard. Mater. 109 (2004) 85–93.

Faisal M., Tariq M.A., Muneer M., Photocatalyzed degradation of two selected dyes in UV-irradiated aqueous suspensions of titania, Dyes Pigments 72 (2007) 233–239.

Fu M., Li Y., Wu S., Lu P., Liu J., Dong F., "Sol–gel preparation and enhanced photocatalytic performance of Cu-doped ZnO nanoparticles", Applied Surface Science 258 (2011) 1587– 1591.

Fujishima, A., Rao, T. N., and Tryk, D. A." TiO_2 photocatalysts and diamond electrodes" Electrochemical Acta 45 (2000) 4683-4690.

Ghule A.V., Lo B., Tzing S.H., Ghule K., Chang H., Ling Y.C., "Simultaneous thermogravimetric analysis and in situ thermo-Raman spectroscopic investigation of thermal decomposition of zinc acetate dehydrate forming zinc oxide nanoparticles", Chemical Physics Letters 381 (2003) 262–270.

Gupta A.K., Pal A., Sahoo C., "Photocatalytic degradation of a mixture of crystal violet (basic violet 3) and methyl red dye in aqueous suspensions using Ag^+ doped TiO_2", Dyes Pigments 69 (2006) 224–232.

Gupta J., Barick K.C., Bahadur D., "Defect mediated photocatalytic activity in shape-controlled ZnO nanostructures", Journal of Alloys and Compounds 509 (2011) 6725–6730.

Hamedani N.F.and Farzaneh F.,"Synthesis of ZnO Nanocrystals with Hexagonal (Wurtzite) Structure in Water Using Microwave Irradiation", Journal of Sciences, Islamic Republic of Iran 17 (2006) 231-234.

Hasnat M.A., Uddin M.M., Samed A.J.F., Alam S.S., Hossain S., "Adsorption and photocatalytic decolorization of a synthetic dye erythrosine on anatase TiO2 and ZnO surfaces", Journal of Hazardous Materials 147 (2007) 471–477.

Jamil T.S., Ghaly M.Y., Fathy N.A., Abd el-halim T.A., Osterlund L., "Enhancement of TiO_2 behavior on photocatalytic oxidation of MO dye using TiO_2/AC under visible irradiation and sunlight radiation", Separation and Purification Technology 98 (2012) 270–279.

Jayalakshmi M., Palaniappa M., Balasubramanian K., "Single Step Solution Combustion Synthesis of ZnO/carbon Composite and its Electrochemical Characterization for Supercapacitor Application", Int. J. Electrochem. Sci., 3 (2008) 96 – 103

Jesionowski T., Kołodziejczak-Radzimska A., Ciesielczyk F., Sójka-Ledakowicz J., Olczyk J., Sielski J., "Synthesis of Zinc Oxide in an Emulsion System and its Depositionon PES Nonwoven Fabric", FIBRES & TEXTILES in Eastern Europe 2011, Vol. 19, No. 2 (85).

Jia X., Fan H., Afzaal M., Wu X., O'Brien P., "Solid state synthesis of tin-doped ZnO at room temperature: Characterization and its enhanced gas sensing and photocatalytic properties", Journal of Hazardous Materials 193 (2011) 194– 199.

Jiang Y., Sun Y., Liu H., Zhu F., Yin H., "Solar photocatalytic decolorization of C.I. Basic Blue 41 in an aqueous suspension of TiO2-ZnO", Dyes and Pigments 78 (2008) 77-83.

Juang R.S., Lin S.H., Hsueh P.Y., "Removal of binary azo dyes from water by UV-irradiated degradation in TiO2 suspensions", Journal of Hazardous Materials 182 (2010) 820–826.

Kaneva N.V., Dimitrov D.T., Dushkin C.D., "Effect of nickel doping on the photocatalytic activity of ZnO thin films under UV and visible light", Applied Surface Science 257 (2011) 8113–8120.

Kazuhito Hashimoto, H. I., Akira Fujishima (2005). "TiO2 Photocatalysis: A Historical Overview and Future Prospects." Japanese Journal of Applied Physics 44(12): 8269-8285.

Khataee A.R., Zarei M., “Photoelectrocatalytic decolorization of di-azo dye by zinc oxide nanophotocatalyst and carbon nanotube based cathode: Determination of the degradation products”, Journal of Desalination 278 (2011) 117–125.

Khorramfar S., Mahmoodi N.M., Arami M., Bahrami H., “Oxidation of dyes from colored wastewater using activated carbon/hydrogen peroxide”, Desalination 279 (2011) 183–189.

Kong J., Li A., Zhai H., Gong Y., Li H., Wu D., “Preparation, characterization of the Ta-doped ZnO nanoparticles and their photocatalytic activity under visible-light illumination”, Journal of Solid State Chemistry 182 (2009) 2061–2067.

Krishnakumar B., Swaminathan M., “Influence of operational parameters on photocatalytic degradation of a genotoxic azo dye Acid Violet 7 in aqueous ZnO suspensions”, Spectrochimica Acta Part A 81 (2011) 739– 744.

Liao S., Donggen H., Yu D., Su Y., Yuan G., “Preparation and characterization of ZnO/TiO2, SO42−/ZnO/TiO2 photocatalyst and their photocatalysis”, Journal of Photochemistry and Photobiology A: Chemistry 168 (2004) 7–13.

Lu C., Wu Y., Mai F., Chung W., Wu C., Lin W., Chen C., “Degradation efficiencies and mechanisms of the ZnO-mediated photocatalytic degradation of Basic Blue 11 under visible light irradiation”, Journal of Molecular Catalysis A: Chemical 310 (2009) 159-165.

Lucas M.S., Peres J.A., “Decolorization of the azo dye Reactive Black 5 by Fenton and photo-Fenton oxidation”, Dyes and Pigments 71 (2006) 236e244.

Mahmood M.A., Baruah S., Dutta J., “Enhanced visible light photocatalysis by manganese doping or rapid”, Materials Chemistry and Physics 130 (2011) 531– 535.

Mohamed R. M., Mkhalid I. A., Baeissa E. S., Al-Rayyani1 M. A., “Photocatalytic Degradation of Methylene Blue by Fe/ZnO/SiO2 Nanoparticles under Visible light”, Journal of Nanotechnology Volume 2012, Article ID 329082, 5 pages doi:10.1155/2012/329082.

Nagaraja R., Kottam N., Girija C.R., Nagabhushana B.M., "Photocatalytic degradation of Rhodamine B dye under UV/solar light using ZnO nanopowder synthesized by solution combustion route", Journal of Powder Technology 215-216 (2012) 91–97.

Nair M.G., Nirmala M., Rekha, K., Anukaliani A., "Structural, optical, photo catalytic and antibacterial activity of ZnO and Co doped ZnO nanoparticles", Materials Letters 65 (2011) 1797–1800.

Neill C. O', Lopez A., Esteves S., Hawkes F.R., Hawkes D.L., Wilcox S., "Azo-dye degradation in an anaerobic–aerobic treatment system operating on simulated textile effluent", Applied Microbiology and Biotechnology 53 (2000) 249–254.

Nenavathu B.P., Rao A.V.R.K., Goyal A., Kapoor A., "Synthesis, characterization and enhanced photocatalytic degradation efficiency of Se doped ZnO nanoparticles using trypan blue as a model dye", Applied Catalysis A: General 459 (2013) 106– 113.

Nilamadanthai A., Sobana N., Subash B., Swaminathan M., Shanthi M., "Photocatalytic destruction of an organic dye, acid red 73 in aqueous ZnO suspension using UV light energy", Indian journal of chemistry 52A (2013) 63-67.

Nishio J., Tokumura M., Znad H.T., Kawase Y., "Photocatalytic decolorization of azo-dye with zinc oxide powder in an external UV light irradiation slurry photoreactor", Journal of Hazardous Materials B138 (2006) 106–115.

P. Rajaguru, K. Kalaiselvi, M. Palanivel, V. Subburam, Biodegradation of azo dyes in a sequential anaerobic–aerobic system, Applied Microbiology and Biotechnology 54 (2000) 268–273.

Pandit P. and B a s u S., "Removal of Ionic Dyes from Waterby Solvent Extraction Using Reverse Micelles", Environ. Sci. Technol. 38 (2004) 2435-2442.

Pare B., Jonnalagadda S.B., Tomar H., Singh P., Bhagwat V.W., "ZnO assisted photocatalytic degradation of acridine orange in aqueous solution using visible irradiation", Desalination 232 (2008) 80–90.

Parvin T., Keerthiraj N., Ibrahim I.A., Phanichphant S., Byrappa K., “Photocatalytic Degradation of Municipal Wastewater and Brilliant Blue Dye Using Hydrothermally Synthesized Surface-Modified Silver-Doped ZnO Designer Particles”, International Journal of Photoenergy,Volume 10 (2012) 610-670.

Pera-Titus, M., Garc´ıa-Molina, V., Ba˜nos, M. A., Jim´enez, J. and Espulgas S. “Degradation of chlorophenols by means of advanced oxidation processes: a general review”. Applied Catalysis B: Environmental 47, 219-156.

Potti P.R. and Srivastava V.C., “Comparative Studies on Structural, Optical, and Textural Properties of Combustion Derived ZnO Prepared Using Various Fuels and Their Photocatalytic Activity”, Ind. Eng. Chem. Res. 2012, 51, 7948−7956.

Pung S.Y., Lee W.P., Aziz A., “Kinetic Study of Organic Dye Degradation Using ZnO Particles with DifferentMorphologies as a Photocatalyst”, International Journal of Inorganic Chemistry,Volume 2012, Article ID 608183, 9 pages;doi:10.1155/2012/608183.

Qiu R., Zhang D., Mo Y., Song L., Brewer E., Huang X., Xiong Y., “Photocatalytic activity of polymer-modified ZnO under visible light irradiation”, Journal of Hazardous Materials 156 (2008) 80–85.

Rajeshwar K., Osugi M.E., Chanmanee W., Chenthamarakshan C.R., Zanoni M.V.B., Kajitvichyanukul P., Krishnan-Ayer R., “Heterogeneous photocatalytic treatment of organic dyes in air and aqueous media”, Journal of Photochemistry and Photobiology C: Photochemistry Reviews 9 (2008) 171–192.

Raoufi D., “Synthesis and microstructural properties of ZnO nanoparticles prepared by precipitation method”, Renewable Energy 50 (2013) 932e937.

Razali M.H., Ali E.D.G.C.E., Kasah M., Omar A.H., "EFFECTS OF CALCINATION TEMPERATURE ONSURFACE MORPHOLOGY AND PHOTOCATALYTIC ACTIVITYOF zno PHOTOCATALYST”, http://www.academia.edu.

Reli M., Koci K., Matejka V., Kovar P., ObalovaL., “EFFECT OF CALCINATION TEMPERATURE AND CALCINATION TIME ON THE KAOLINITE/TiO_2

COMPOSITE FOR PHOTOCATALYTIC REDUCTION OF CO_2", GeoScience Engineering, Volume LVIII (2012), No.4, p. 10-22, ISSN 1802-5420.

Riaz N., Chong F.K., Dutta B.K., Man Z.B., Khan M.S., Nurlaela E., "Photodegradation of Orange II under visible light using Cu–Ni/TiO2: Effect of calcination temperature", Chemical Engineering Journal 185– 186 (2012) 108– 119.

S. Meric, D. Kaptan, T. Olmez, Color and COD removal from wastewater containing reactive black 5 using Fenton's oxidation process, Chemosphere 54 (2004) 435–441.

Sanchez J.V., Orozco J.P.P., Parra R.S., Perez I.H., "DEGRADATION OF REACTIVE RED 120 AZO DYE IN AQUEOUS SOLUTIONS USING HOMOGENEOUS/HETEROGENEOUS IRON SYSTEMS", Revista Mexicana de Ingeniería Química, vol. 11, núm. 1, 2012, pp. 121-131.

Shanthi M., Kuzhalosai V., "Photocatalytic degradation of an azo dye, acid red 27, in aqueous solution using nano ZnO", Indian journal of chemistry,Vol.51A,March 2012,pp. 428-434.

Shi Z., Zhang X., Yao S., "Preparation and photocatalytic activity of TiO2 nanoparticles co-doped with Fe and La", Particuology 9 (2011) 260‑ 264.

Shifu C.,Wei L., Huaye Z., Xiaoling Y., "Photocatalytic decolorization of soluble dyes by a bis-ions coexistence system of NH_4^+ and NO_3^- with high photoreduction ability", Journal of Hazardous Materials 186 (2011) 1687–1695.

Shinde S.S., Bhosale C.H., Rajpure K.Y., "Oxidative degradation of acid orange 7 using Ag-doped zinc oxide thin films", Journal of Photochemistry and Photobiology B: Biology 117 (2012) 262–268.

Shinde S.S., Bhosale C.H., Rajpure K.Y., "Photocatalytic degradation of toluene using sprayed N-doped ZnO thin films in aqueous suspension", Journal of Photochemistry and Photobiology B: Biology 113 (2012) 70–77.

Silva C.G., Wang W., Faria J.L., "Photocatalytic and photochemical degradation of mono-, di- and tri-azo dyes in aqueous solution under UV irradiation", J. Photochem. Photobiol. A: Chem. 181 (2006) 314–324.

Sivasankar B., Sadasivam V., "Kinetic studies on the photocatalytic degradation of direct yellow 12 in the presence of ZnO catalyst", Journal of Molecular catalysis A:Chemical,306,77-81.

Sn-doped Chalcopyrites with Wide-spectrum Solar Response", Sci. Rep. 3, 1286; DOI:10.1038/

Sobana N. and Swaminathan M., "Combination effect of ZnO and activated carbon for solar assisted photocatalytic degradation of Direct Blue 53", Solar Energy Materials & Solar Cells 91 (2007) 727–734.

Sobana N., Swaminathan M.2007[b], "The effect of operational parameters on the photocatalytic degradation of acid red 18 by ZnO", Separation and Purification Technology 56 (2007) 101–107.

srep01286 (2013).

Srivastava V.C., Mall I.D., Mishra I.M., "Adsorption of toxic metal ions onto activated carbon Study of sorption behaviour through characterization and kinetics", Chemical Engineering and Processing 47 (2008) 1275‑1286.

Sun J., Dong S., Feng J., Yin X., Zhao X., "Enhanced sunlight photocatalytic performance of Sn-doped ZnO for Methylene Blue degradation", Journal of Molecular Catalysis A: Chemical 335 (2011) 145–150.

Sun J.H., Dong S.Y., Feng J.L., Yin X.J., Zhao X.C., "Enhanced sunlight photocatalytic performance of Sn-doped ZnO for Methylene Blue degradation", Journal of Molecular Catalysis A: Chemical 335 (2011) 145‑150.

Sweeny E. A., Chipman J.K., Forsythe S.J., "Evidence for Direct-acting Oxidative Genotoxicity by Reduction Products of Azo Dyes", Environ Health Perspect. 1994 October; 102: 119–122.

Tekbas M., Yatmaz H.C., Bektas N., "Heterogeneous photo-Fenton oxidation of reactive azo dye solutions using iron exchanged zeolite as a catalyst", Microporous and Mesoporous Materials 115 (2008) 594–602.

Velmurugan R., Swaminathan M., "An efficient nanostructured ZnO for dye sensitized degradation of Reactive Red 120 dye under solar light",Journal of Solar Energy Materials & Solar Cells 95 (2011) 942–95.

Wang J., Fan X.M., Tian K., Zhou Z.W., Wang Y., "Largely improved photocatalytic properties of Ag/tetrapod-like ZnO nanocompounds prepared with different PEG contents", Applied Surface Science 257 (2011) 7763–7770.

Wang J., Li C.,Luan X., Li J., Wang B., Zhang L., Xu R., Zhang X., "Investigation on solar photocatalytic activity of TiO_2 loaded composite: TiO_2/Skeleton, TiO_2/Dens and TiO_2/HAP", Journal of Molecular Catalysis A: Chemical 320 (2010) 62–67.

Wang J., Li J., Xie Y., Li C., Han G., Zhang L., Xu R., Zhang X., "Investigation on solar photocatalytic degradation of various dyes in the presence of Er3+:YAlO3/ZnO–TiO2 composite", Journal of Environmental Management 91 (2010) 677–684.

Wang J., Li J., Xie Y., Zhang Z., Li J., Chen X., Zhang L., Xu R., Zhang X., "Photocatalytic degradation of organic dyes with Er^{3+}:$YAlO_3$/ZnO composite under solarlight", Solar Energy Materials & Solar Cells 93 (2009) 355–361.

Wang J., Xie Y., Zhang Z., Li J., Li D., Zhang L., Xing Z., Xu R., Zhang X., "Photocatalytic degradation of organic dyes by Er^{3+}:$YAlO_3$/TiO_2 composite under solar light", Environ Chem Lett (2010) 8:87–93,DOI 10.1007/s10311-008-0196-4.

Wang L., Egerton T., "The Effect of Transition Metal on the Optical Properties and Photoactivity of Nano-particulate Titanium Dioxide", Journal of Materials Science Research;Vol. 1, No. 4; 2012.

Welderfael T., Yadav O.P., Taddesse A.M., Kaushal J., "Synthesis, characterization and photocatalytic activities of Ag-N-codoped ZnO nanoparticles for degradation of methyl red", Bull. Chem. Soc. Ethiop. 2013, 27(2), 221-232.

Wu C., Shen L., Zhang Y., Huang Q., "Solvothermal synthesis of Cr-doped ZnO nanowires with visible light-driven photocatalytic activity", Materials Letters 65 (2011) 1794–1796.

Wu C.,S. L., Zhang Y.C.,Huang Q., " Synthesis of AgBr/ZnO nanocomposite with visible light driven photocatalytic activity , Journal of materials letter ,66(2012)83-85.

Xu Y.,Xu H., Li H., Xia J., Liu C., Liu L., "Enhanced photocatalytic activity of new photocatalyst Ag/AgCl/ZnO", Journal of Alloys and Compounds 509 (2011) 3286–3292.

Yang C., Qin M., Wang Y., Wan D., Huang F., Lin J., "Observation of an Intermediate Band in

Yazdanbakhsh M., Khosravi I., Goharshadi E. K., Youssefi A., "Fabrication of nanospinel ZnCr2O4 using sol–gel method and its application on removal of azo dye from aqueous solution", Journal of Hazardous Materials 184 (2010) 684–689.

Yuan M., Wang S., Wang X., Zhao L., Hao T., "Removal of organic dye by air and macroporous ZnO/MoO3/SiO2 hybrid under room conditions", Applied Surface Science 257 (2011) 7913–7919.

Zhai J., Tao X., Pu Y., Zeng X., Chen J., "Core/shell structured ZnO/SiO2 nanoparticles: Preparation, characterization and photocatalytic property", Applied Surface Science 257 (2010) 393–397.

Zhao L., Ran J., Shu Z., Dai G., Zhai P., Wang S.' "Effects of Calcination Temperatures on Photocatalytic Activity of Ordered Titanate Nanoribbon/SnO_2 Films Fabricated during an EPD Process", International Journal of Photoenergy ,Volume 2012 (2012), Article ID 472958, 7 pages, doi:10.1155/2012/472958.